bioRxiv preprint doi: https://doi.org/10.1101/386581; this version posted August 7, 2018. The copyright holder for this preprint (which was not certified by peer review) is the author/funder, who has granted bioRxiv a license to display the preprint in perpetuity. It is made available under aCC-BY-NC-ND 4.0 International license.

Identification, Genotyping, and Pathogenicity of *Trichosporon* spp. Isolated from Giant Pandas

Xiaoping Ma[1#], Yaozhang Jiang[1#], Chengdong Wang[2]*, Yu Gu[3]*, Sanjie Cao[1], Xiaobo Huang[1], Yiping Wen[1], Qin Zhao[1], Rui Wu[1], Xintian Wen[1], Qigui Yan[1], Xinfeng Han[1], Zhicai Zuo[1], Junliang Deng[1], Zhihua Ren[1], Shumin Yu[1], Liuhong Shen[1], Zhijun Zhong[1], Guangneng Peng[1], Haifeng Liu[1] , Ziyao Zhou[1]

[1]Key Laboratory of Animal Disease and Human Health of Sichuan Province , College of Veterinary Medicine, Sichuan Agricultural University, Chengdu, 611130, China;

[2] China Conservation and Research Center for the Giant Panda, Ya'an, Sichuan 625000, China.

[3] College of Life Sciences, Sichuan Agricultural University, Chengdu, 611130, China.

***Co-corresponding authors:**

ChengdongWang: 285934012@qq.com

Yu Gu: 23985202@qq.com;

[#]**These authors contributed equally to this work and are co-first authors.**

The methods were carried out in accordance with the approved guidelines.

All animal experiments were approved by the Sichuan Agricultural University animal ethics committee.

bioRxiv preprint doi: https://doi.org/10.1101/386581; this version posted August 7, 2018. The copyright holder for this preprint (which was not certified by peer review) is the author/funder, who has granted bioRxiv a license to display the preprint in perpetuity. It is made available under aCC-BY-NC-ND 4.0 International license.

ABSTRACT

Trichosporon is the dominant genus of epidermal fungi in giant pandas and causes local and deep infections. To provide the information needed for the diagnosis and treatment of trichosporosis in giant pandas, the sequence of ITS, D1/D2, and IGS1 loci in 29 isolates of *Trichosporon* spp. which isolated from the body surface of giant pandas were combination to investigate interspecies identification and genotype. Morphological development was examined via slide culture. Additionally, mice were infected by skin inunction, intraperitoneal injection, and subcutaneous injection for evaluation of pathogenicity. The twenty-nine isolates of *Trichosporon* spp. were identified as belonging to 11 species, and *Trichosporon jirovecii* and *T. asteroides* were the commonest species. Four strains of *T. laibachii* and one strain of *T. moniliiforme* were found to be of novel genotypes, and *T. jirovecii* was identified to be genotype 1. *T. asteroides* had the same genotype which involved in disseminated trichosporosis. The morphological development processes of the *Trichosporon* spp. were clearly different, especially in the processes of single-spore development. Pathogenicity studies showed that 7 species damaged the liver and skin in mice, and their pathogenicity was stronger than other 4 species. *T. asteroides* had the strongest pathogenicity and might provoke invasive infection. The pathological characteristics of liver and skin infections caused by different *Trichosporon* spp. were similar.

So it is necessary to identify the species of *Trichosporon* on the surface of giant panda. Combination of ITS, D1/D2, and IGS1 loci analysis, and morphological development process can effectively identify the genotype of *Trichosporon* spp.

bioRxiv preprint doi: https://doi.org/10.1101/386581; this version posted August 7, 2018. The copyright holder for this preprint (which was not certified by peer review) is the author/funder, who has granted bioRxiv a license to display the preprint in perpetuity. It is made available under aCC-BY-NC-ND 4.0 International license.

Keywords: *Trichosporon*; ITS； D1/D2； IGS1； identification; Morphology; Pathogenicity

1. Introduction

Trichosporon is a genus of fungi that belongs to the order *Tremellales* in the class *Tremellomycetes* (division *Basidiomycota*) and is widely distributed in nature(1). *Trichosporon* spp. can cause superficial fungal infections such as tinea pedis, onychomycosis, and dermoid infections(2). With the increasing prevalence of immunocompromised patients, the incidence of invasive fungal diseases has increased, and *Trichosporon* has become the second commonest genus of yeast fungus in deep fungal infections in patients with hematologic malignancies, granulocytic deficiency, and bone marrow transplants(3). Owing to difficulties in the classification and identification of *Trichosporon* spp., studies of invasive fungal infections have substantially lagged behind those of other species in areas such as clinical characteristics, antifungal susceptibilities, and the selection of therapeutic drugs, and this has become a difficult problem in the study of fungal infections(4).

Trichosporon spp. mainly cause skin and organ granuloma, and related pathogenicity studies have focused on *Trichosporon* spp. that colonize humans, such as *Trichosporon asahii*, *T. asteroides*, *T. inkin*, and *T. dermatis*. In recent years, reports of trichosporosis in animals have increased. Some cases in animals have been reported in the last decade, such as disseminated trichosporosis in cats(5), canine meningitis(6), and tortoise shell infection(7). A study described a case of systemic infection by *T. loubieri* in a cat with acute dyspnea, anorexia, and aggressive behavior; a cutaneous biopsy from ulcerated wounds revealed necrogranulomatous dermatitis and

bioRxiv preprint doi: https://doi.org/10.1101/386581; this version posted August 7, 2018. The copyright holder for this preprint (which was not certified by peer review) is the author/funder, who has granted bioRxiv a license to display the preprint in perpetuity. It is made available under aCC-BY-NC-ND 4.0 International license.

65 panniculitis with numerous intralesional fungal hyphae(5).

66 To enable accurate identification of *Trichosporon* spp., a number of molecular
67 methods have been developed, of which DNA sequencing of the internal transcribed
68 spacer (ITS) region, the D1/D2 domain of the 26S subunit of the rRNA gene region,
69 and the intergenic spacer 1 (IGS1) region are the most frequently used. The IGS1
70 gene region has been particularly useful in phylogenetic studies and the description of
71 intraspecies variation(8, 9). Ribeiro et al. identified 21 clinical isolates as belonging to
72 six species on the basis of the ITS and IGS1 regions(10).

73 In 2009, Chagasneto et al. identified 22 isolates from human blood by analyzing the
74 IGS1 region(11). In 2011, Guo identified 29 clinical isolates of *Trichosporon* by
75 analyzing 3 loci, and eight *Trichosporon* spp. were found, of which *T. asahii* was the
76 commonest(9). Identification of multiple *Trichosporon* spp. isolated from animals has
77 not been reported. In addition, *Trichosporon* spp. are the dominant fungal species on
78 panda skin(12). The identification at the species level is important for preventing
79 dermatomycoses in giant pandas and improving related research.

80 At present, there have been few studies of the morphology of *Trichosporon* spp. In
81 2005, Li performed slide culture of six clinically common *Trichosporon* spp. and
82 found no significant differences in colony morphology(13).

83 We collected 29 isolates of *Trichosporon* spp. from the skin of giant pandas at the
84 China Conservation and Research Center for Giant Pandas, Ya'an. Owing to the
85 shortage of sequence data for the IGS1 region in individual species, we had to analyze
86 the ITS region, D1/D2 domain, and IGS1 region of the isolates to obtain accurate

bioRxiv preprint doi: https://doi.org/10.1101/386581; this version posted August 7, 2018. The copyright holder for this preprint (which was not certified by peer review) is the author/funder, who has granted bioRxiv a license to display the preprint in perpetuity. It is made available under aCC-BY-NC-ND 4.0 International license.

87 classification information. Afterward, the morphological development process was
88 observed by the slide culture method. Mice were artificially infected, and their livers
89 and skin were taken for pathological analysis.

90 **2. Materials and methods**

91 **2.1 Sampling procedure**

92 Samples were collected from clinically healthy giant pandas (22 females and 22
93 males) at the China Conservation and Research Center for Giant Pandas (Ya'an,
94 China) in 2015–2016. Pandas that had been treated with antifungal drugs during the
95 previous 6 months or with a recent history of disease were excluded from this study.
96 The pandas lived in a semi-captive semi-enclosed breeding environment, were fed a
97 diet of about 10% steamed cornbread and fruits and 90% bamboo shoots, and were
98 allowed to drink water *ad libitum*(14).

99 All personnel involved in sampling wore sterile protective clothing, hats, masks,
100 and latex gloves. When a panda ate fruits, 70% alcohol was used to sterilize the
101 surface of the dorsal forearm, and then a suitable amount of dander was collected
102 using sterilized surgical blades, scissors, and forceps. All samples were quickly placed
103 in sterilized plastic sample bags, transported to the laboratory on ice within 2 h, and
104 then immediately processed in a BSL-2 safety cabinet. No repeat sampling was
105 performed on the same panda, and all 44 samples were processed with isolated
106 *Trichosporon* spp.(14).

107 **2.2 Fungal culture**

bioRxiv preprint doi: https://doi.org/10.1101/386581; this version posted August 7, 2018. The copyright holder for this preprint (which was not certified by peer review) is the author/funder, who has granted bioRxiv a license to display the preprint in perpetuity. It is made available under aCC-BY-NC-ND 4.0 International license.

Samples were streak-inoculated under aerobic conditions onto Sabouraud dextrose agar (SDA) (MOLTOX, Inc., Boone, NC) containing 4% (m/v) glucose, 1% (m/v) peptone, and 1.5% (m/v) agar. All media were supplemented with the antibiotics cycloheximide (0.05%, m/v) and chloramphenicol (0.005%, m/v).

Fungal culture was carried out in a BSL-2 safety cabinet in a bioclean room. Sterilized sealing film was used to cover each plate. Each sample was plated onto three culture plates with three control plates. All culture dishes were inoculated and stored at 25 °C for 7–30 days before being considered negative(14).

2.3 Molecular identification

Fungal DNA was extracted from pure culture isolates as described previously(15). Amplification of the ITS region, D1/D2 domain, and IGS1 region was performed as described with the primer pairs ITS1/ITS4 (ITS1: 5'-TCCGTAGGTGAACCTGCGG-3'; ITS4: 5'-TCCTCCGCTTATTGATATGC-3'), F63/R635 (F63: 5'-GCATATCAATAAGCGGAGCAAAAG-3'; R635: 5'-GGTCCGTGTTTCAAGACG-3'), and 26SF/5SR (26SF: 5'-ATCCTTTGCAGACGACTTGA-3'; 5SR: 5'-AGCTTGACTTCGCAGATCGG-3'), respectively[8, 16]. PCR amplification was performed in a 50 µl reaction mixture containing 19 µl 2 × Taq Master Mix (Tsingke Biotech Co., Ltd., Chengdu, China), 2 µl primers, 25 µl double-distilled water, and 2 µl fungal genomic DNA. The thermocycling conditions were as follows: 5 min at 98 °C (initial denaturation), 35 cycles of 10 s at 98 °C, 10 s at 58 °C, and extension at 72 °C for 10 s, and final extension for 4 min at 72 °C. A total of 8 µl of the amplified

bioRxiv preprint doi: https://doi.org/10.1101/386581; this version posted August 7, 2018. The copyright holder for this preprint (which was not certified by peer review) is the author/funder, who has granted bioRxiv a license to display the preprint in perpetuity. It is made available under aCC-BY-NC-ND 4.0 International license.

PCR products were visualized on 2% agarose gel after staining with GreenView (Solarbio, Beijing). The PCR products were then sequenced by Tsingke Biotech Co., Ltd. (Chengdu, China).

All the chromatograms of DNA sequences were examined to ensure high-quality sequences. For species identification, the sequences of the ITS region, D1/D2 domain, and IGS1 region were queried against the NCBI database (https://www.ncbi.nlm.nih.gov). The sequence of each locus and concatenated sequences were then aligned using the NCBI BLAST and formed the consensus sequences for all 29 isolates. Phylogenetic trees were computed with MEGA version 6 (Molecular Evolutionary Genetic Analysis software version 6.0.2; http://www.megasoftware.net) using the neighbor-joining method, in which all positions containing gaps and missing data were eliminated from the dataset. The ITS region plus the D1/D2 domain and IGS1 region were used to produce two separate phylogenetic trees. All sequences of the three genes from the 29 isolates were deposited in the GenBank database (https://www.ncbi.nlm.nih.gov/genbank/) and were assigned ID numbers (Table 1).

2.4 Morphological development process

All 29 isolates were identified as *Trichosporon* spp. after molecular identification. Microscopic observations of the 29 isolates were made after slide culture on SDA(1). A 0.5 ml sample of melted medium was injected into a closed glass Petri dish, which comprised a slide glass, a cover glass, and a copper ring with a hole in the wall, and was inoculated via the hole(17, 18). All isolates were incubated at 25 °C and were

bioRxiv preprint doi: https://doi.org/10.1101/386581; this version posted August 7, 2018. The copyright holder for this preprint (which was not certified by peer review) is the author/funder, who has granted bioRxiv a license to display the preprint in perpetuity. It is made available under aCC-BY-NC-ND 4.0 International license.

152 observed after 24, 48, 72 and 96 h. The cover glass was stained with 5 ml cotton blue
153 (Hopebio, Qingdao) and was observed with a microscope (BX51, Olympus).

154 **2.5 Pathogenicity experiment**

155 **2.5.1 Animal experiment**

156 Each *Trichosporon* sp. was inoculated by skin inunction (We abraded skin with emery
157 paper until a slight bleedingand cut the hair (2 cm×2 cm) on the back of mouse after
158 anesthesia by diethyl ether), subcutaneous injection, and intraperitoneal injection into
159 immunosuppressed and non-immunosuppressed mice. In total, six groups were used,
160 each of which comprised three mice. Groups A (intraperitoneal injection), B
161 (subcutaneous injection), and C (skin inunction) were immunosuppressed（Mice were
162 given intraperitoneal injection with 50 mg/kg cyclophosphamide at intervals of 48
163 hours, three times in total, and each mouse was given 15 mg of penicillin sodium
164 under the skin.）; groups D (intraperitoneal injection), E (subcutaneous injection), and
165 F (skin inunction) were non-immunosuppressed. In totalof 216 sex-matched SPF
166 Kunming mice (Dashuo Science and Technology Co., Ltd., China), which belonged to
167 11 experiment groups and one control group, with ages of 6–8 weeks were used.

168 **2.5.2 Preparation of fungal suspension and inoculation**

169 Before being inoculated, mice in the immunosuppressed groups were
170 intraperitoneally injected with *Trichosporon* spp. that had been cultured in SDA at
171 25 °C for 5 d. The mycelium and spores were scraped, washed with physiological
172 saline, and mixed well. A hemocytometer was used to adjust the concentration of the
173 spore suspension to 1×10^7 CFU/ml. Except in the control group, each mouse was

bioRxiv preprint doi: https://doi.org/10.1101/386581; this version posted August 7, 2018. The copyright holder for this preprint (which was not certified by peer review) is the author/funder, who has granted bioRxiv a license to display the preprint in perpetuity. It is made available under aCC-BY-NC-ND 4.0 International license.

174 inoculated with 0.1 ml fungal suspension. Mice in the control group received 0.1 ml
175 physiological saline instead. The backs of the mice treated by skin inunction were
176 shaved, sterilized with 75% (w/w) alcohol, and lightly abraded with a 25G needle, and
177 then 0.1 ml fungal suspension was gently rubbed onto the skin with a sterile injector.

178 **2.5.3 Tissue sample processing**

179 The diet and clinical symptoms of the mice were observed daily. The mice were
180 anesthetized with 5 ml diethyl ether (Chengdu Kelong Chemical Reagent Factory),
181 decapitated, and dissected to observe lesions on the seventh day after infection. The
182 livers of mice in groups A and D and skin lesions from mice in the other groups were
183 taken for fungal culture and pathological evaluation. The livers and skin were placed
184 in 100 ml 4% formalin (Chengdu Kelong Chemical Reagent Factory; 500 ml w/w) for
185 histopathological study via staining with hematoxylin/eosin and periodic acid/Schiff
186 stain(6).

187 **3. Results**

188 **3.1 Molecular identification and genotyping**

189 The interspecies identification of 22 isolates of *Trichosporon* spp. was performed
190 from the data in Fig. 1. Seven strains of *Trichosporon* (JYZ1221, JYZ1224, JYZ915,
191 JYZ1223, JYZ1261, JYZ1252, and JYZ12922) could not be identified because of the
192 lack of sequence information for IGS1 in the GenBank database. However, it was
193 determined that these seven *Trichosporon* strains belonged to three species. The
194 interspecies identification of all 29 isolates of *Trichosporon* spp. was performed using
195 the data in Fig. 2. The structures of the two phylogenetic trees were basically identical,

bioRxiv preprint doi: https://doi.org/10.1101/386581; this version posted August 7, 2018. The copyright holder for this preprint (which was not certified by peer review) is the author/funder, who has granted bioRxiv a license to display the preprint in perpetuity. It is made available under aCC-BY-NC-ND 4.0 International license.

196 and the method could be used to determine the accuracy of the identification of the 29
197 isolates. The 29 isolates of *Trichosporon* spp. were identified as belonging to 11
198 species, namely, *T. laibachii* (4 strains), *T. gracile* (1), *T. brassicae* (1), *T. domesticum*
199 (1), *T. guehoae* (3), *T. asteroides* (5), *T. jirovecii* (5), *T. cutaneum* (1), *T. shinodae* (1),
200 *T. middelhovenii* (3), and *T. moniliiforme* (4). *T. jirovecii* and *T. asteroides* were the
201 commonest species (17%, 5/29). Moreover, *T. middelhovenii* and *T. shinodae* were
202 isolated from the surfaces of animals for the first time.

203 In this study, preliminary genotyping was performed on *Trichosporon* spp. *T.*
204 *asteroides* (JYZ1251, JYZ1281, JYZ371, JYZ1255, and JYZ951) had the same
205 genotype as its reference strain, which was isolated from the blood of
206 immunocompromised patients(11), whereas *T. laibachii* (JYZ3252, JYZ921, JYZ321,
207 and JYZ912) had different genotypes. The reference strain was isolated from humans.
208 The five isolates of *T. jirovecii* were identified as having genotype 1(9). *T. brassicae*
209 (JYZ1253) had the same genotype as the reference strain, which was isolated from
210 cabbage(8). *T. gracile* (JYZ1291) had the same genotype as the reference strain,
211 which was isolated from spoiled milk(8). *T. domesticum* (JYZ983) and the reference
212 strain had the same genotype; the reference strain was isolated from human sputum(8).
213 Three strains of *T. moniliiforme* (JYZ932, JYZ331, and JYZ323) had the same
214 genotype as the reference strain, which was isolated from curdling milk(8), but the
215 strain JYZ372 did not have this genotype. It was difficult to determine whether *T.*
216 *cutaneum* had the same genotype as the reference strain. According to the
217 phylogenetic tree, the genetic relationship was distant and it may not have had the

bioRxiv preprint doi: https://doi.org/10.1101/386581; this version posted August 7, 2018. The copyright holder for this preprint (which was not certified by peer review) is the author/funder, who has granted bioRxiv a license to display the preprint in perpetuity. It is made available under aCC-BY-NC-ND 4.0 International license.

same genotype.

3.2 Morphological development process

The morphological development processes of the *Trichosporon* spp. were clearly different, and the difference was significant for the processes of single-spore development. Spores of *T. moniliiforme* and *T. shinodae* tended to be self-replicating at the beginning of their development and reproduced mainly by budding. Spores of the other species tended to become mycelia and reproduced mainly by the differentiation of mycelia to form spores or produce arthrospores. Morphological development could be used as an important basis for the identification of *Trichosporon* spp. For example, *T. moniliiforme* produced a large number of spores, and the spores were transformed into an oval shape after development was completed. The growth of *T. shinodae* was the slowest among the *Trichosporon* spp.; the shape of mycelia was specific and served as a basis for identification. *T. laibachii* produced a large number of arthrospores and had the unique feature that the mycelia were folded together. The main method of growth of *T. guehoae* comprised the reproduction of arthrospores by budding, and it had the specific feature that new mycelia grew from gaps in segmented mycelia. The morphological appearances of *T. brassicae*, *T. domesticum* and *T. gracile* were analogous in some ways. All these *Trichosporon* spp. tended to reproduce via the differentiation of mycelia into spores, and few arthrospores were seen during the process of development. The shapes of spores that differentiated from mycelia were different: those of *T. gracile* were quadrilateral, those of *T. domesticum* were round, and those of *T. brassicae* were disciform. The

bioRxiv preprint doi: https://doi.org/10.1101/386581; this version posted August 7, 2018. The copyright holder for this preprint (which was not certified by peer review) is the author/funder, who has granted bioRxiv a license to display the preprint in perpetuity. It is made available under aCC-BY-NC-ND 4.0 International license.

arthrospores of *T. middelhovenii* were fusiform and were always located in a bifurcation of the mycelium. This characteristic was distinct from other *Trichosporon* spp. *T. asteroides* had the feature that the spores overlapped each other, and the mycelia were thin and short. The mycelia could differentiate into spores, and the pigmentation of the spores was uneven, as shown by dyeing with cotton blue. The morphologies of *T. jirovecii* and *T. cutaneum* were similar, but the mycelia of *T. cutaneum* were more curved and tended to differentiate into spores, in contrast to *T. jirovecii*. *Trichosporon* spp. have individual morphological characteristics and hence could be distinguished by means of a comparison of their morphological development processes.

After culture for 24 h, spores of *T. moniliiforme* divided independently (Fig. 3A), no hyphae differentiated into spores (Fig. 3B, C, and D), and the mycelium and spores were evenly stained (Fig. 3B, C, and D). The mycelium produced a large number of arthrospores (Fig. 3C), and the shape of the spores changed from circular (Fig. 3C) to elliptical (Fig. 3D).

The spores of *T. laibachii* grew into mycelium after cultivation for 24 h, and no spores divided independently (Fig. 4A). The mycelium spread radially (Fig. 4A) and was folded together (Fig. 4C), and differentiated into spores. Arthrospores were abundant, whereas spores were round and few in number (Fig. 4B, C, and D). The spores and mycelium were unevenly colored: the spores were darker, whereas the mycelium was lighter (Fig. 4B, C, and D). Hyphal folding was typical in structure.

The structural development of *T. guehoae* was completed after cultivation for 24 h

bioRxiv preprint doi: https://doi.org/10.1101/386581; this version posted August 7, 2018. The copyright holder for this preprint (which was not certified by peer review) is the author/funder, who has granted bioRxiv a license to display the preprint in perpetuity. It is made available under aCC-BY-NC-ND 4.0 International license.

(Fig. 5A). The mycelium spread radially but was scattered (Fig. 5A, B, C, and D). A large number of round spores were produced as grape-like clusters (Fig. 5A, B, and C). Hyphae and spores were evenly stained (Fig. 5A, B, C, and D). The mycelium grew from a segmented section to form a new mycelium (Fig. 5B), and the new spores were generated by arthrospores (Fig. 5D); this was a typical structure.

After *T. gracile* was cultured for 24 h, a large amount of hyphae appeared and became segmented, and no spores could be seen (Fig. 6A). It could be seen that the mycelium differentiated into spores (Fig. 6B, C and D). A large number of spores were produced, which were mostly square (Fig. 6C) and became oval after reaching maturity (Fig. 6D). The mycelia and spores were evenly stained (Fig. 6C). Some hyphae did not divide into sections and differentiated into spores at intervals; this was a typical structure (Fig. 6D).

After culture for 24 h, the spores of *T. domesticum* swelled to form mycelia and no spores divided independently (Fig. 7A). Hyphae were abundant and parallel to each other and had spindle-type buds (Fig. 7B). A large number of hyphae differentiated into spores (Fig. 7C and D). The number of spores was small with no arthrospores, and the spores were round (Fig. 7B, C, and D). The mycelia and spores were evenly stained (Fig. 7A, B, C, and D).

After culture for 24 h, the spores of *T. brassicae* exhibited no significant changes (Fig. 8A), whereas after culture for 48 h the spores swelled and formed hyphae (Fig. 8B). No spores were found to divide independently (Fig. 8A and B). The mycelia became segmented and were distributed parallel to each other (Fig. 8C). It could be

bioRxiv preprint doi: https://doi.org/10.1101/386581; this version posted August 7, 2018. The copyright holder for this preprint (which was not certified by peer review) is the author/funder, who has granted bioRxiv a license to display the preprint in perpetuity. It is made available under aCC-BY-NC-ND 4.0 International license.

284 seen that the mycelium differentiated into spindle-shaped spores (Fig. 8D). The
285 mycelium and spores were evenly stained (Fig. 8D), and there were few arthrospores
286 (Fig. 8C).

287 After cultivation for 24 h, some spores of *T. shinodae* swelled (Fig. 9A), whereas
288 other spores divided independently (Fig. 9B). The hyphae were short and sparse and
289 grew very slowly (Fig. 9C). A large number of round arthrospores were produced (Fig.
290 9D). The spores and mycelium were evenly colored (Fig. 9C and D). Crude short
291 mycelium was produced after culture for 72 h (Fig. 9C); this was a typical structure.

292 After culture for 24 h, *T. asteroides* formed slender hyphae, and no spores divided
293 independently (Fig. 10A). The mycelium was elongated (Fig. 10C) and could
294 differentiate into spores (Fig. 10B and D). Spores on bifurcated mycelium aggregated
295 into spheres (Fig. 10C); a large number of spores were produced, and the spores were
296 round, oval, or spindle-shaped (Fig. 10B and D). The spores were not evenly
297 pigmented and some were dark in color (Fig. 10D). The bifurcation of the mycelia
298 and the aggregation of spores into spheres were typical structures (Fig. 10C).

299 After *T. middelhovenii* was cultivated for 24 h, hyphae were generated and no
300 spores were found to divide independently (Fig. 11A). The hyphae were elongated
301 (Fig. 11A and D), and their segments were small and indistinct (Fig. 11B and D). No
302 hyphae differentiated into spores. Spores at bifurcations were spindle-shaped (Fig.
303 11A, B, C, and D). The spores were few in number and darker (Fig. 11C and D).
304 Shuttle-type articular spores were characteristic structures (Fig. 11A, B, C, and D).

305 After *T. jirovecii* was cultivated for 24 h, hyphae appeared and no spores were seen

bioRxiv preprint doi: https://doi.org/10.1101/386581; this version posted August 7, 2018. The copyright holder for this preprint (which was not certified by peer review) is the author/funder, who has granted bioRxiv a license to display the preprint in perpetuity. It is made available under aCC-BY-NC-ND 4.0 International license.

306 to divide independently (Fig. 12A). The hyphae were segmented and radial (Fig. 12A)
307 and differentiated into spores (Fig. 12D). Arthrospores were round and large in
308 number (Fig. 12B); mycelia and spores were uniformly colored (Fig. 12D).

309 After cultivation for 24 h, spores of *T. cutaneum* swelled and budded, and some
310 spores divided independently (Fig. 13A). The mycelium was curved and segmented
311 (Fig. 13B and C) and differentiated into spores (Fig. 13D). A large number of round
312 arthrospores (Fig. 13C) were produced. The mycelium and spores were evenly stained
313 (Fig. 13D), and curved mycelium was a typical structure (Fig. 13B and D).

314 **3.3 Pathogenicity**

315 The results of this study indicated that *Trichosporon* spp. mostly caused necrosis or
316 swelling of hepatocytes and enlargement of the inter-hepatocyte space, and necrosis of
317 hepatocytes mostly occurred near liver vessels. Subcutaneous injection of
318 *Trichosporon* spp. caused lymphocyte infiltration into the skin, abscesses, and
319 thickening of the stratum corneum. Mice that were inoculated via skin inunction had
320 no obvious lesions, and most of them exhibited changes in the thickness of the
321 stratum corneum, which in some cases resulted in subcutaneous abscesses. Tissues
322 infected with *Trichosporon* spp. have a strong tendency to bleed, which causes
323 congestion in both the skin and the liver. Most of the *Trichosporon* spp. caused
324 significant damage to the liver and skin, for example, *T. laibachii*, *T. brassicae*, *T.*
325 *guehoae*, *T. asteroides*, *T. jirovecii*, *T. cutaneum*, *T. shinodae*, and *T. middelhovenii*. *T.*
326 *asteroides*, *T. laibachii*, *T. brassicae*, *T. guehoae*, *T. cutaneum*, *T. shinodae*, and *T.*
327 *middelhovenii* all produced spores in the skin infection model (Fig.S1~S10). In

bioRxiv preprint doi: https://doi.org/10.1101/386581; this version posted August 7, 2018. The copyright holder for this preprint (which was not certified by peer review) is the author/funder, who has granted bioRxiv a license to display the preprint in perpetuity. It is made available under aCC-BY-NC-ND 4.0 International license.

328 particular, *T. asteroides* gave rise to disseminated infections in the reticular layer of
329 the skin (Fig. 14G1) and budding in the dermis (Fig. 14G2). *T. gracile*, *T.*
330 *moniliiforme*, and *T. domesticum* caused inconspicuous pathological changes, and
331 hence their pathogenicity was weak.

332 **4. Discussion**

333 **4.1 Interspecies identification of *Trichosporon* spp.**

334 There have been reports on the isolation and identification of fungi from the body
335 surface of the giant panda(12). It was concluded that *Trichosporon* spp. were the
336 dominant genus among skin flora on the giant panda(12). Recently, there have been
337 many reports on infections by *T. asahii*(19-24), but few mentions of other
338 *Trichosporon* spp.(6, 25). However, there have been reports that some animals are
339 susceptible to rare *Trichosporon* spp.(25-27). Because the phylogenetic relationship
340 between *Trichosporon* spp. was very close, it was impossible to distinguish the
341 different species of *Trichosporon* spp. according to the ITS region or D1/D2 domain
342 in every case(28). The sequence similarity between the ITS regions of *T. asahii* and *T.*
343 *asteroides*, in which only two or three bases are different, is 99–99.3%, and *T.*
344 *montevideense* and *T. domesticum* have identical ITS regions(29). Scorzetti *et al*.
345 found that the differences between the 28s rDNA D1/D2 domains of different
346 *Trichosporon* spp. are greater than those between the corresponding ITS regions. The
347 ITS regions of *T. laibachii* and *T. multisporum* are identical, and seven bases are
348 different in the D1/D2 domains. Two bases are different in the D1/D2 domains of *T.*
349 *montevideense* and *T. domesticum*(30). Guo amplified all three loci (ITS, D1/D2, and

bioRxiv preprint doi: https://doi.org/10.1101/386581; this version posted August 7, 2018. The copyright holder for this preprint (which was not certified by peer review) is the author/funder, who has granted bioRxiv a license to display the preprint in perpetuity. It is made available under aCC-BY-NC-ND 4.0 International license.

IGS1) and constructed a phylogenetic tree for the ITS region and D1/D2 domain and a separate phylogenetic tree for the IGS1 region. Both trees could completely distinguish the *Trichosporon* spp.(9). In this study, seven strains could not be identified by their IGS1 regions because of the lack of sequence information for IGS1 in the NCBI database. Hence, we used the joint contribution of the ITS region and D1/D2 domain, which we compared with the phylogenetic tree for IGS1. It was found that the clades of the phylogenetic trees were basically identical and authenticated each other, so that all 29 strains could be identified completely.

4.2 Pathogenicity of dominant *Trichosporon* spp. isolated from pandas

T. asteroides and *T. jirovecii* were the dominant *Trichosporon* spp. that were isolated from the giant panda samples, and these species are widely present in giant pandas(12). Their pathogenicity has a great influence on the health of giant pandas(12). In this study, the reference strain of *T. asteroides* was isolated from the blood of patients with disseminated infections caused by *Trichosporon* spp.(11), which indicated high pathogenicity. *T. jirovecii* genotype 1 has been isolated from the human body(9), but its pathogenicity was unknown. Thus far, there have been few reports on *T. jirovecii*: Malgorzata et al. reported one case of mixed respiratory infection in a dog caused by *T. jirovecii* and *Rhodotorula*(31, 32), and Nardoni reported one case of back infection in a tortoise caused by *T. jirovecii*(7). In this study, four strains of *T. laibachii* (JYZ3252, JYZ921, JYZ321, and JYZ912) and one strain of *T. moniliiforme* (JYZ372) were identified as having new genotypes. Their pathogenicity remains to be confirmed by future studies.

bioRxiv preprint doi: https://doi.org/10.1101/386581; this version posted August 7, 2018. The copyright holder for this preprint (which was not certified by peer review) is the author/funder, who has granted bioRxiv a license to display the preprint in perpetuity. It is made available under aCC-BY-NC-ND 4.0 International license.

4.3 Genotyping of *Trichosporon* spp.

At present, IGS1 sequence analysis is generally used for genotyping *Trichosporon* spp. For example, Chagasneto et al. completed the genotyping of 14 strains of *T. asahii* by IGS sequence analysis(11), whereas Guo completed the genotyping of 39 strains of *T. asahii*(8). The main target in the genotyping of *Trichosporon* spp. has been *T. asahii,* and the genotyping of other *Trichosporon* spp. has been rare. In this study, among all the isolates only *T. jirovecii* had been assigned to two genotypes, and the other species had not been studied(9). The main reason was that the identification of *Trichosporon* spp. is difficult and sequence information for IGS1 is scarce. In this study, only preliminary genotyping was performed for *Trichosporon* spp., and further research will rely on improvements in sequence information for IGS1in *Trichosporon* spp.

4.4 Morphological development process of *Trichosporon* spp.

There have been few studies on the morphology of *Trichosporon* spp. In 2005, Li et al. performed ITS-PCR detection and morphological and susceptibility testing on six *Trichosporon* spp.(13). The colonies of different *Trichosporon* spp. were similar, but the morphologies of their mycelia and spores were significantly different. The structure of the mycelium was not destroyed, and the test results were credible. The morphology of the mycelia of *T. domesticum* was very similar to that in this study. The morphological development process of *Trichosporon* spp. was significantly different, and the majority of *Trichosporon* spp. had a typical structure: for example, septal differentiation of the mycelium in *T. gracile* (Fig. 8D); short thick mycelium

bioRxiv preprint doi: https://doi.org/10.1101/386581; this version posted August 7, 2018. The copyright holder for this preprint (which was not certified by peer review) is the author/funder, who has granted bioRxiv a license to display the preprint in perpetuity. It is made available under aCC-BY-NC-ND 4.0 International license.

394 during the development of *T. shinodae* (Fig. 11C); elongation and bifurcation of the
395 mycelium and the aggregation of spores into spheres in *T. asteroides* (as shown in Fig.
396 10C); and a spindle-type articular spore structure in *T. middelhovenii* (Fig. 13A, B, C,
397 and D). The above results proved that the morphological development process and
398 typical structure have great significance as references for morphological
399 identification.

400 From the point of view of the development and sporulation of mycelia,
401 *Trichosporon* is an intermediate genus between molds and yeasts. Its mycelia can
402 differentiate into a large number of spores like yeasts and also produce conidia like
403 molds. Spores in the early stages of development can either bud like hyphae or divide
404 like those of yeasts. Colonies of some *Trichosporon* spp. resemble yeasts in being
405 milky, oily, and reflective, whereas colonies of some *Trichosporon* spp. have a radiate
406 texture similar to that of molds(13). *Trichosporon* might represent an intermediate
407 genus in the evolution of yeasts into molds. In the study of the morphology of
408 *Trichosporon* spp., they should be regarded as molds in order to observe their
409 sporulation and mycelial structure.

410 **4.5 Pathological changes in *Trichosporon* spp. infections**

411 Different *Trichosporon* spp. cause similar pathological lesions on the skin and liver. *T.*
412 *asahii* caused hepatic sinusoidal dilatation, mild to moderate dilatation of small blood
413 vessels, hyperemia, neutrophil-based focal infiltration of inflammatory cells, and
414 proliferation or degeneration of hepatocytes(33). *T. dermatis* caused hepatic
415 sinusoidal dilatation and congestion, swelling, degeneration, or necrosis of

bioRxiv preprint doi: https://doi.org/10.1101/386581; this version posted August 7, 2018. The copyright holder for this preprint (which was not certified by peer review) is the author/funder, who has granted bioRxiv a license to display the preprint in perpetuity. It is made available under aCC-BY-NC-ND 4.0 International license.

hepatocytes, and hyperplasia of Kupffer cells(34). These lesions were similar to the pathological changes in the liver observed in this study. In the literature there are few mentions of skin lesions, subcutaneous abscesses, and bruises that were caused by *T. dermatis*.

However, most of the *Trichosporon* spp. identified in this study could cause skin lymphocyte infiltration, abscesses, and thickening of the stratum corneum.The pathological changes were significantly different between the groups treated by subcutaneous injection and skin inunction. These conclusions were similar to those of a study that was reported in China for the first time in 2010(35). The skin damage caused in the group treated by skin inunction was lighter, and only *T. laibachii* and *T. asteroides* caused obvious pathological changes, which might be related to the uncontrollable amount of the spore coating and the pathogenicity of the *Trichosporon* spp. themselves. The spores developed a strong tendency to form mycelium, and the process of formation of mycelium could cause mechanical damage, which might be a reason for these observations.

4.6 Pathogenicity of the *Trichosporon* spp.

Except for *T. moniliiforme*, *T. domesticum*, and *T. gracile*, all the *Trichosporon* spp. in this study caused significant damage to the liver and skin in healthy mice (Fig.S1~S10). In most cases spores stained with periodic acid/Schiff stain could be observed in skin sections. *T. brassicae*, *T. guehoae*, *T. middelhovenii*, and *T. shinodae* were found for the first time to be pathogenic forms of *Trichosporon* that could provoke obvious lesions in immunosuppressed and non-immunosuppressed groups.

bioRxiv preprint doi: https://doi.org/10.1101/386581; this version posted August 7, 2018. The copyright holder for this preprint (which was not certified by peer review) is the author/funder, who has granted bioRxiv a license to display the preprint in perpetuity. It is made available under aCC-BY-NC-ND 4.0 International license.

Hitherto, reports of the pathogenicity of these four *Trichosporon* spp. had not been found. This might be related to difficulties in the identification of *Trichosporon* spp. and differences in pathogenicity caused by the differences between strains.

In this study, *T. asteroides* (JYZ1255) exhibited strong pathogenicity. The infected tissue was extensively congested, and there was a large area of abscess. Two mice in group A died 2 days after being inoculated with a suspension of *T. asteroides*. There have been many reports on *T. asteroides*, which is one of the main pathogens involved in trichosporosis in humans and is a dominant strain among fungi on the body surface of the giant panda. *T. asteroides* caused purulent keratitis(36) and was also isolated from the blood of patients with disseminated trichosporosis(9, 11). *T. asteroides* gave rise to obvious disseminated infections in the reticular layer of the skin (Fig. 14G1) and budding in the dermis (Fig. 14G2). The infections might cause damage or even be life-threatening to immunocompromised giant pandas. *T. jirovecii* (JYZA10) was identified as having genotype 1 in previous studies (Fig. 1) and was significantly more pathogenic in immunosuppressed mice than in non-immunosuppressed mice and tissue. The degree of damage was significantly lower than that caused by *T. asteroides*, and it was inferred that genotype 1 of *T. jirovecii* was opportunistically pathogenic. Four strains of *T. laibachii* were identified as having new genotypes by phylogenetic analysis of the IGS1 sequence (Fig. 2). Although there have currently been no reported cases of infection involving *T. laibachii*, *T. laibachii* (JYZ3252) caused skin ulceration in mice (Fig. 4). This lesion demonstrated that the new genotype of *T. laibachii* is more pathogenic.

bioRxiv preprint doi: https://doi.org/10.1101/386581; this version posted August 7, 2018. The copyright holder for this preprint (which was not certified by peer review) is the author/funder, who has granted bioRxiv a license to display the preprint in perpetuity. It is made available under aCC-BY-NC-ND 4.0 International license.

The pathogenicity test only studied the effects of *Trichosporon* spp. on the skin and liver, and most of the isolated *Trichosporon* spp. caused more severe damage to skin than to the liver. For example, *T. brassicae* (JYZ1253) and the reference strain, which was isolated from rancid milk, had the same genotype, but the isolated strain caused severe inflammatory reactions in skin tissue and skin necrosis. *T. asteroides* (JYZ1255) and the reference strain, which was isolated from human blood, had the same genotype, but the isolated strain caused disseminated infections in the reticular layer of the skin. It was assumed that the pathogenicity of *Trichosporon* spp. is related to their parasitic environment and that *Trichosporon* spp. that are isolated from the skin surface cause more pronounced damage to the skin.

List of abbreviations

There are no abbreviations.

Declarations

Ethics approval and consent to participants

All animal experiments were approved by the Institutional Animal Care and Use Committee of the Sichuan Agricultural University (permit number DYY-S20151326). Permissions were obtained from the China Conservation and Research Center for the Giant Panda Breeding prior to sample collection from the pandas.

Consent for publication

Not applicable

Competing interests

bioRxiv preprint doi: https://doi.org/10.1101/386581; this version posted August 7, 2018. The copyright holder for this preprint (which was not certified by peer review) is the author/funder, who has granted bioRxiv a license to display the preprint in perpetuity. It is made available under aCC-BY-NC-ND 4.0 International license.

The authors declare that they have no competing interests

Funding

This study was supported by the Applied Basic Research Project in Sichuan Province (2018JY0183), and international cooperation funds for giant pandas (AD1415).

Authors' contributions

XM，YJ,CW,YG,SC,XH YW,QZ,RW,QY and XH carried out the collection of the sample of the giant pandas, isolated fungi, conceived the study, and drafted the manuscript. ZZ, JD, ZR, SY, LS and GP participated in the sequence alignment, carried out the molecular genetic studies, and participated in the data analysis. HL and ZZconceived the study, participated in its design and coordination, and helped draft the manuscript. All authors read and approved the final manuscript.

Acknowledgements

Refercence

1. Wang DL. 2005. Medical mycology. People's Medical Publishing House.
2. Kim ES, Kim DH, Chang SE, Lee MW, Choi JH, Sung KJ, Moon KC, Koh JK. 2003. Trichosporon species in onychomycosis and tinea pedis. Korean Journal of Dermatology 41:702-707.
3. Denning DW, Evans EGV, Kibbler CC, Richardson MD, Roberts MM, Rogers TR, Warnock DW, Warren RE. 1997. Guidelines for the investigation of invasive fungal infections in haematological malignancy and solid organ transplantation. European Journal of Clinical Microbiology & Infectious Diseases 16:424-436.
4. Girmenia C, Pagano L, Martino B, D'Antonio D, Fanci R, Specchia G, Melillo L, Buelli M, Pizzarelli G, Venditti M. 2005. Invasive infections caused by Trichosporon species and Geotrichum capitatum in patients with hematological malignancies: a retrospective multicenter study from Italy and review of the literature. Journal of Clinical Microbiology 43:1818-28.
5. Rissi DR, Kirby KD, Sanchez S. 2016. Systemic Trichosporon loubieri infection in a cat. Journal of Veterinary Diagnostic Investigation Official Publication of the American Association of Veterinary Laboratory Diagnosticians Inc 28.

bioRxiv preprint doi: https://doi.org/10.1101/386581; this version posted August 7, 2018. The copyright holder for this preprint (which was not certified by peer review) is the author/funder, who has granted bioRxiv a license to display the preprint in perpetuity. It is made available under aCC-BY-NC-ND 4.0 International license.

6. Bryan LK, Porter BF, Wickes BL, Spaulding KA, Kerwin SC, Lawhon SD. 2014. Meningoencephalitis in a Dog Due to Trichosporon montevideense. Journal of Comparative Pathology 151:157-161.
7. Nardoni S, Salvadori M, Poli A, Rocchigiani G, Mancianti F. 2017. Cutaneous lesions due to Trichosporon jirovecii in a tortoise (Testudo hermanni). Medical Mycology Case Reports 18:18.
8. Sugita T, Nakajima M, Ikeda R, Matsushima T, Shinoda T. 2002. Sequence Analysis of the Ribosomal DNA Intergenic Spacer 1 Regions of Trichosporon Species. Journal of Clinical Microbiology 40:1826-30.
9. Guo L-N, Xiao M, Kong F, Chen SCA, Wang H, Sorrell TC, Jiang W, Dou H-T, Li R-Y, Xu Y-C. 2011. Three-Locus Identification, Genotyping, and Antifungal Susceptibilities of Medically Important Trichosporon Species from China. Journal of Clinical Microbiology 49:3805-3811.
10. Ribeiro MA, Alastruey-Izquierdo A, Gomez-Lopez A, Rodriguez-Tudela JL, Cuenca-Estrella M. 2008. Identificación molecular y sensibilidad a los antifúngicos de cepas de Trichosporon aisladas en un hospital de Brasil. Revista Iberoamericana De Micología 25:221-225.
11. Chagas-Neto TC, Chaves GM, Melo ASA, Colombo AL. 2009. Bloodstream Infections Due to Trichosporon spp.: Species Distribution, Trichosporon asahii Genotypes Determined on the Basis of Ribosomal DNA Intergenic Spacer 1 Sequencing, and Antifungal Susceptibility Testing. Journal of Clinical Microbiology 47:1074-1081.
12. Xiaoping M, qi X, desheng L. 2016. Isolation, identification and phylogenetic analysis of culturable fungi in hair of Ailuropoda melanoleuca. Chinese Veterinary Science 1:72-81.
13. Li HM, Du HT, Liu W, Wan Z, Li RY. 2005. Microbiological characteristics of medically important Trichosporon species. Mycopathologia 160:217-25.
14. Ma X, Li C, Hou J, Yu G. 2017. Isolation and identification of culturable fungi from the genitals and semen of healthy giant pandas (Ailuropoda melanoleuca). Bmc Veterinary Research 13:344.
15. Makimura K, Murayama SY, Yamaguchi H. 1994. Detection of a wide range of medically important fungi by the polymerase chain reaction. Journal of Medical Microbiology 40:358-364.
16. Diaz MR, Fell JW. 2004. High-Throughput Detection of Pathogenic Yeasts of the Genus Trichosporon. Journal of Clinical Microbiology 42:3696.
17. Song Q, Zhou H, Lai X. 2013. Clinical application of identification of fungal strains by copper coil culture. Journal of Jiujiang University (Natural Science Edition) 28:76-77.
18. Feng P, Lu Q, Najafzadeh MJ, Gerrits van den Ende AHG, Sun J, Li R, Xi L, Vicente VA, Lai W, Lu C, de Hoog GS. 2012. Cyphellophora and its relatives in Phialophora: biodiversity and possible role in human infection. Fungal Diversity 65:17-45.
19. Fournier S, Pavageau W, Feuillhade M, Deplus S, Zagdanski AM, Verola O, Dombret H, Molina JM. 2002. Use of voriconazole to successfully treat disseminated Trichosporon asahii infection in a patient with acute myeloid leukaemia. European Journal of Clinical Microbiology & Infectious Diseases Official Publication of the European Society of Clinical Microbiology 21:892-896.
20. Meyer MH, Letscherbru V, Waller J, Lutz P, Marcellin L, Herbrecht R. 2002. Chronic disseminated Trichosporon asahii infection in a leukemic child. Clinical Infectious Diseases An Official Publication of the Infectious Diseases Society of America 35:e22.

bioRxiv preprint doi: https://doi.org/10.1101/386581; this version posted August 7, 2018. The copyright holder for this preprint (which was not certified by peer review) is the author/funder, who has granted bioRxiv a license to display the preprint in perpetuity. It is made available under aCC-BY-NC-ND 4.0 International license.

21. Bassetti M, Bisio F, Di BA, Pierri I, Balocco M, Soro O, Cruciani M, Bassetti D. 2004. Trichosporon asahii infection treated with caspofungin combined with liposomal amphotericin B. Journal of Antimicrobial Chemotherapy 54:575-7.
22. Ghiasian SA, Maghsood AH, Mirhendi SH. 2006. Disseminated, fatal Trichosporon asahii infection in a bone marrow transplant recipient. Journal of microbiology, immunology, and infection = Wei mian yu gan ran za zhi 39:426.
23. Nakajima M, Sugita T, Y. 2007. Granuloma associated with Trichosporon asahii infection in the lung: Unusual pathological findings and PCR detection of Trichosporon DNA. Medical Mycology 45:641-644.
24. Gross JW, Kan VL. 2008. Trichosporon asahii infection in an advanced AIDS patient and literature review. Aids 22:793-5.
25. Rissi DR, Kirby KD, Sanchez S. 2016. Systemic Trichosporon loubieri infection in a cat. J Vet Diagn Invest 28:350-3.
26. Bieganska MJ, Rzewuska M, Dabrowska I, Malewska-Biel B, Ostrzeszewicz M, Dworecka-Kaszak B. 2018. Mixed Infection of Respiratory Tract in a Dog Caused by Rhodotorula mucilaginosa and Trichosporon jirovecii: A Case Report. Mycopathologia 183:637-644.
27. Ueda K, Nakamura I, Itano EN, Takemura K, Nakazato Y, Sano A. 2017. Trichosporon asteroides Isolated from Cutaneous Lesions of a Suspected Case of "paracoccidioidomycosis ceti" in a Bottlenose Dolphin (Tursiops truncatus). Mycopathologia 182:937-946.
28. Gunn SR, Reveles XT, Hamlington JD, Sadkowski LC, Johnsonpais TL, Jorgensen JH. 2006. Use of DNA Sequencing Analysis To Confirm Fungemia Due to Trichosporon dermatis in a Pediatric Patient. Journal of Clinical Microbiology 44:1175.
29. Sugita T, Nishikawa A, Ikeda R, Shinoda T. 1999. Identification of Medically Relevant Trichosporon Species Based on Sequences of Internal Transcribed Spacer Regions and Construction of a Database for Trichosporon Identification. Journal of Clinical Microbiology 37:1985-93.
30. Scorzetti G, Fell JW, Fonseca A, Statzelltallman A. 2003. Systematics of basidiomycetous yeasts: a comparison of large subunit D1/D2 and internal transcribed spacer rDNA regions. Fems Yeast Research 3:495-517.
31. Rodrigueztudela JL, Diazguerra TM, Mellado E, Cano V, Tapia C, Perkins A, Gomezlopez A, Rodero L, Cuencaestrella M. 2005. Susceptibility Patterns and Molecular Identification of Trichosporon Species. Antimicrobial Agents & Chemotherapy 49:4026.
32. Biegańska MJ, Rzewuska M, Dąbrowska I, Malewska-Biel B, Ostrzeszewicz M, Dworecka-Kaszak B. 2017. Mixed Infection of Respiratory Tract in a Dog Caused by Rhodotorula mucilaginosa and Trichosporon jirovecii : A Case Report. Mycopathologia:1-8.
33. Montoya AM, Lunarodríguez CE, Treviñorangel RJ, Becerrilgarcía M, Ballesteroselizondo RG, Saucedocárdenas O, González GM. 2017. In vivo pathogenicity of Trichosporon asahii isolates with different in vitro enzymatic profiles in an immunocompetent murine model of systemic trichosporonosis. Medical Mycology:1-8.
34. Lin Y-P. 2011. Mouse pathogenicity of *Trichosporon dermatis* and clinical and mycoligical study of *Exophiala spinifera*-induced phaeohyphmycosisGuangdong Medical College.
35. Xia Z, Yang R. 2010. Trichosporosis. Practical Journal of Dermatology 03:215-217.
36. Fang Y, Wang Q, Tang Z. 2008. Clinical analysis of 80 cases of suppurative keratitis. Journal of

bioRxiv preprint doi: https://doi.org/10.1101/386581; this version posted August 7, 2018. The copyright holder for this preprint (which was not certified by peer review) is the author/funder, who has granted bioRxiv a license to display the preprint in perpetuity. It is made available under aCC-BY-NC-ND 4.0 International license.

599 Luzhou Medical College 31:91-92.

600

601

Table 1 *Nucleotide sequence accession numbers.*

Strain	Molecular Identification	IGS1 blast	ITS GenBank Accession Number	D1/D2 GenBank Accession Number	IGS1 GenBank Accession Number
JYZ3252	*T. laibachii*	*T. laibachii*	KX302021	MG708435	MG708464
JYZ921	*T. laibachii*	*T. laibachii*	KX034345	MG708441	MG708470
JYZ321	*T. laibachii*	*T. laibachii*	KX302022	MG708433	MG708462
JYZ912	*T. laibachii*	*T. laibachii*	KX034344	MG708439	MG708468
JYZ1291	*T. gracile*	*T. gracile*	KX302008	MG708454	MG708483
JYZ1253	*T. brassicae*	*T. brassicae*	KX302047	MG708450	MG708479
JYZ983	*T. domesticum*	*T. domesticum*	KX034390	MG708444	MG708473
JYZ1221	*T. guehoae*	*Trichosporon* sp.	KX302031	MG708445	MG708474
JYZ1224	*T. guehoae*	*Trichosporon* sp.	KX302081	MG708447	MG708476
JYZ915	*T. guehoae*	*Trichosporon* sp.	KX034350	MG708440	MG708469
JYZ1251	*T. asteroides*	*T. asteroides*	KX302012	MG708448	MG708477
JYZ1281	*T. asteroides*	*T. asteroides*	KX302074	MG708453	MG708482
JYZ371	*T. asteroides*	*T. asteroides*	KX302060	MG708437	MG708466
JYZ1255	*T. asteroides*	*T. asteroides*	KX302051	MG708451	MG708480
JYZ951	*T. asteroides*	*T. asteroides*	KX034347	MG708443	MG708472
JYZA10	*T. jirovecii*	*T. jirovecii*	MG857660	MG708460	MG708489
JYZA5	*T. jirovecii*	*T. jirovecii*	MG857657	MG708457	MG708486
JYZA7	*T. jirovecii*	*T. jirovecii*	MG857658	MG708458	MG708487
JYZA9	*T. jirovecii*	*T. jirovecii*	MG857659	MG708459	MG708488
JYZA12	*T. jirovecii*	*T. jirovecii*	MG857661	MG708461	MG708490
JYZ030202	*T. cutaneum*	*T. cutaneum*	MG857656	MG708456	MG708485
JYZ1223	*T. shinodae*	no result	KX302045	MG708446	MG708475
JYZ1261	*T. middelhovenii*	no result	KX302046	MG708452	MG708481
JYZ1252	*T. middelhovenii*	no result	KX302043	MG708449	MG708478
JYZ12922	*T. middelhovenii*	no result	KX302044	MG708455	MG708484
JYZ932	*T. moniliiforme*	*T. moniliiforme*	KX034371	MG708442	MG708471
JYZ331	*T. moniliiforme*	*T. moniliiforme*	KX302017	MG708436	MG708465
JYZ372	*T. moniliiforme*	*T. moniliiforme*	KX302067	MG708438	MG708467
JYZ323	*T. moniliiforme*	*T. moniliiforme*	KX302018	MG708434	MG708463

Note: Twenty-nine isolates of *Trichosporon* spp. were identified as belonging to 11 species, namely, *T. laibachii* (4 isolates), *T. gracile* (1 isolate), *T. brassicae* (1 isolate), *T. domesticum* (1 isolate), *T. guehoae* (3 isolates), *T. asteroides* (5 isolates), *T. jirovecii* (5 isolates), *T. cutaneum* (1 isolate), *T. shinodae* (1 isolate), *T. middelhovenii* (3 isolates), and *T. moniliiforme* (4 isolates). *T. jirovecii* and *T. asteroides* were the commonest species, each of which accounted for 17% (5/29) of the isolates.

bioRxiv preprint doi: https://doi.org/10.1101/386581; this version posted August 7, 2018. The copyright holder for this preprint (which was not certified by peer review) is the author/funder, who has granted bioRxiv a license to display the preprint in perpetuity. It is made available under aCC-BY-NC-ND 4.0 International license.

Fig. 1 Phylogenetic tree based on IGS1 sequences

Fig. 2 Phylogenetic tree based on ITS sequences plus D1/D2 sequences

Fig. 3 Morphological development process of *Trichosporon moniliiforme* from day 1 to day 4
A: Most spores divided and a small number of spores expanded; B: Scattered hyphae appeared and began to produce conidia on day 2; C: Basic hyphae formed; D: Spores increased in number and their shapes were transformed from circular to elliptical.

Fig. 4 Morphological development process of *Trichosporon laibachii* from day 1 to day 4
A: Some spores germinated and mycelium began to divide; B: Mycelium produced arthrospores; C: Mycelium was folded; D: Mature mycelium and arthrospores.

Fig. 5 Morphological development process of *Trichosporon guehoae* from day 1 to day 4
A: Mycelial buds formed new mycelium; B: New mycelium appeared at the point at which hyphae were segmented; C: A large number of botryoidal spores of *T. guehoae* were observed; D: New spores developed from arthrospores.

Fig. 6 Morphological development process of *Trichosporon gracile* from day 1 to day 4
A and B: Hyphae were segmented; C: A large number of hyphae differentiated into spores, some of which were square; D: Mycelium divided into oval spores.

Fig. 7 Morphological development process of *Trichosporon domesticum* from day 1 to day 4
A: Spores expanded and sprouted; B: Mycelium had multiple branches and spindle-shaped buds; C: Mycelium began to differentiate into oval spores; D: Mycelium had completely differentiated into oval spores.

Fig. 8 Morphological development process of *Trichosporon brassicae* from day 1 to day 4
A: Spindle-shaped spores; B: Spores sprouted; C: Hyphae were segmented and spores were less oval; in the segmented hyphae, the arthrospores were fewer in number and spindle-shaped, and some spores developed into mycelium; D: Hyphae differentiated into spindle-shaped spores.

Fig. 9 Morphological development process of *Trichosporon shinodae* from day 1 to day 4
A: Spores swelled and budded; B: Spores divided; C: Spores formed thick and short hyphae; D: Mycelium produced a large number of arthrospores.

Fig. 10 Morphological development process of *Trichosporon asteroides* from day 1 to day 4
A: Tenuous mycelium, some of which began to become segmented; B: Mycelium differentiated into circular, oval, and spindle-shaped spores; C: The tail ends of mycelium produced a large number of small, aggregating spores and bifurcated; D: Mycelium differentiated into darker spores.

Fig. 11 Morphological development process of *Trichosporon middelhovenii* from day 1 to day 4

bioRxiv preprint doi: https://doi.org/10.1101/386581; this version posted August 7, 2018. The copyright holder for this preprint (which was not certified by peer review) is the author/funder, who has granted bioRxiv a license to display the preprint in perpetuity. It is made available under aCC-BY-NC-ND 4.0 International license.

A: Hyphae were slender and did not divide; B: Hyphae produced fusiform arthrospores; C: Arthrospores budded to form new hyphae; D: Mature mycelium produced a large number of fusiform spores.

Fig. 12 Morphological development process of *Trichosporon jirovecii* from day 1 to day 4

A: Mycelium was slightly segmented and formed arthrospores; B and C: Mycelium formed a large number of circular arthrospores; D: Mycelium differentiated into spores.

Fig. 13 Morphological development process of *Trichosporon cutaneum* from day 1 to day 4

A: Some spores expanded and sprouted, and some spores divided; B: Spores formed curved mycelium; C: Most mycelium was segmented, and the mycelium produced round arthrospores; D: Mycelium began to fold and differentiated into spores.

Fig. 14 Pathological sections of tissue damaged by *Trichosporon asteroides* (JYZ1255) infection

A: Hepatocyte necrosis, hepatic sinusoidal congestion, and unclear hepatic cord structure; B1: Abscess of the dermis, necrosis of muscle tissue, and blood capillary congestion; B2: Epidermis with a large area of blood stasis and abscess; C1: Thickening of granular layer of skin and cuticle; C2: Infiltration of neutrophilic granulocytes into the epidermis; D: Hepatocyte necrosis and hepatic sinusoidal congestion; E1: A large number of neutrophils infiltrated into the reticular layer, muscle tissue, and dermis, and some cells are necrotic; E2: Osteonecrosis of the dermis and hyperplasia of connective tissue; F: Thickening of granular layer of skin and cuticle; G1: Spores stained with periodic acid/Schiff stain (PAS) in the reticular layer of the skin of a mouse in group B; G2: Spores stained with PAS in the dermis and spore germination in a mouse in group B; H: Spores stained with PAS in the dermis of a mouse in group E.

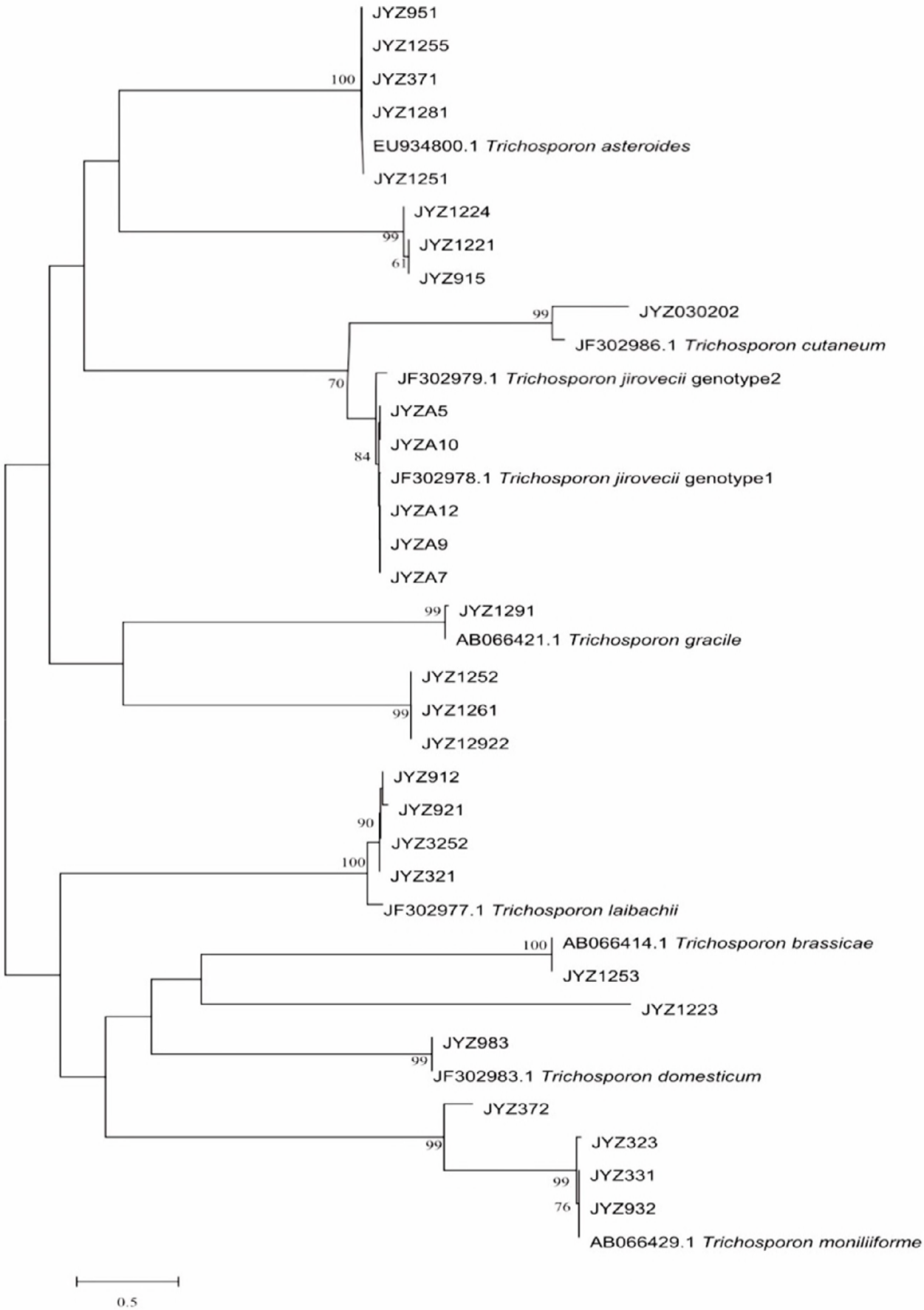
JYZ951
JYZ1255
100
JYZ371
JYZ1281
EU934800.1 Trichosporon asteroides
JYZ1251
JYZ1224
99
JYZ1221
61
JYZ915
99
JYZ030202
JF302986.1 Trichosporon cutaneum
70
JF302979.1 Trichosporon jirovecii genotype2
JYZA5
JYZA10
84
JF302978.1 Trichosporon jirovecii genotype1
JYZA12
JYZA9
JYZA7
99
JYZ1291
AB066421.1 Trichosporon gracile
JYZ1252
99
JYZ1261
JYZ12922
JYZ912
90
JYZ921
JYZ3252
100
JYZ321
JF302977.1 Trichosporon laibachii
100
AB066414.1 Trichosporon brassicae
JYZ1253
JYZ1223
JYZ983
99
JF302983.1 Trichosporon domesticum
JYZ372
99
JYZ323
99
JYZ331
76
JYZ932
AB066429.1 Trichosporon moniliiforme
0.5

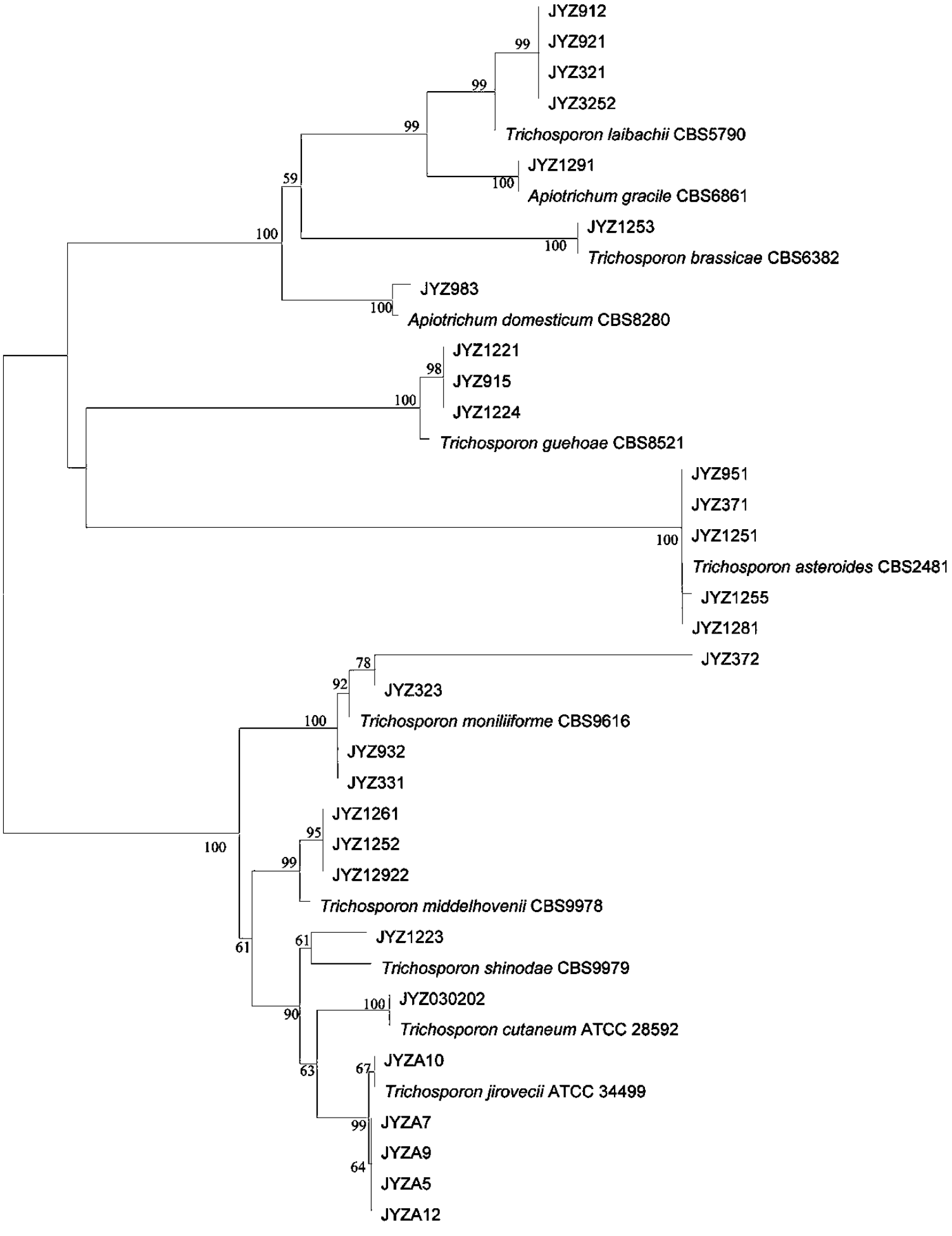
JYZ912
99
JYZ921
JYZ321
99
JYZ3252
99
Trichosporon laibachii CBS5790
JYZ1291
59
100
Apiotrichum gracile CBS6861
JYZ1253
100
100
Trichosporon brassicae CBS6382
JYZ983
100
Apiotrichum domesticum CBS8280
JYZ1221
98
JYZ915
100
JYZ1224
Trichosporon guehoae CBS8521
JYZ951
JYZ371
100
JYZ1251
Trichosporon asteroides CBS2481
JYZ1255
JYZ1281
JYZ372
78
92
JYZ323
Trichosporon moniliiforme CBS9616
100
JYZ932
JYZ331
JYZ1261
95
JYZ1252
100
99
JYZ12922
Trichosporon middelhovenii CBS9978
JYZ1223
61
61
Trichosporon shinodae CBS9979
JYZ030202
100
90
Trichosporon cutaneum ATCC 28592
JYZA10
67
63
Trichosporon jirovecii ATCC 34499
JYZA7
99
JYZA9
64
JYZA5
JYZA12
0.01

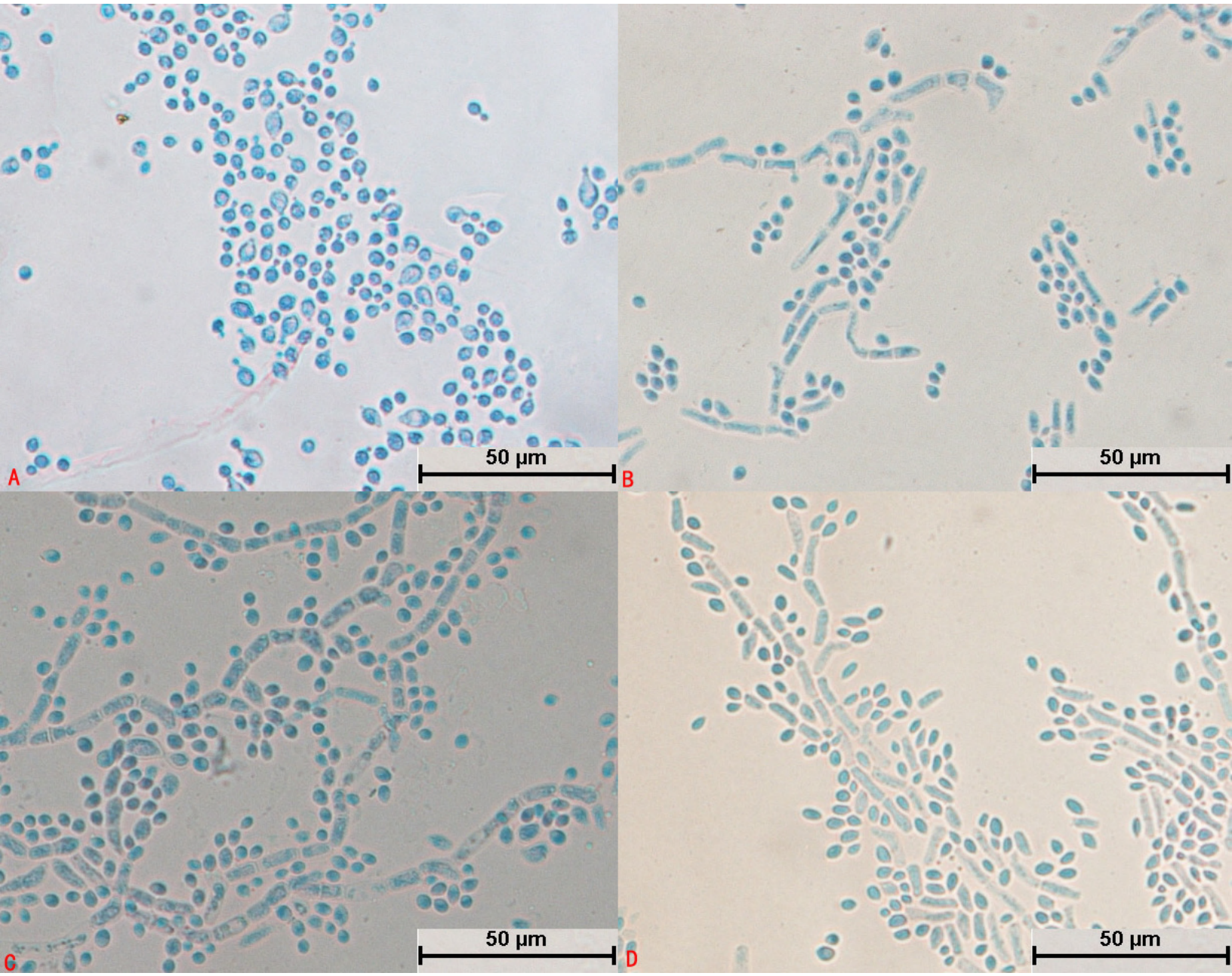
A
50 µm
B
50 µm
C
50 µm
D
50 µm

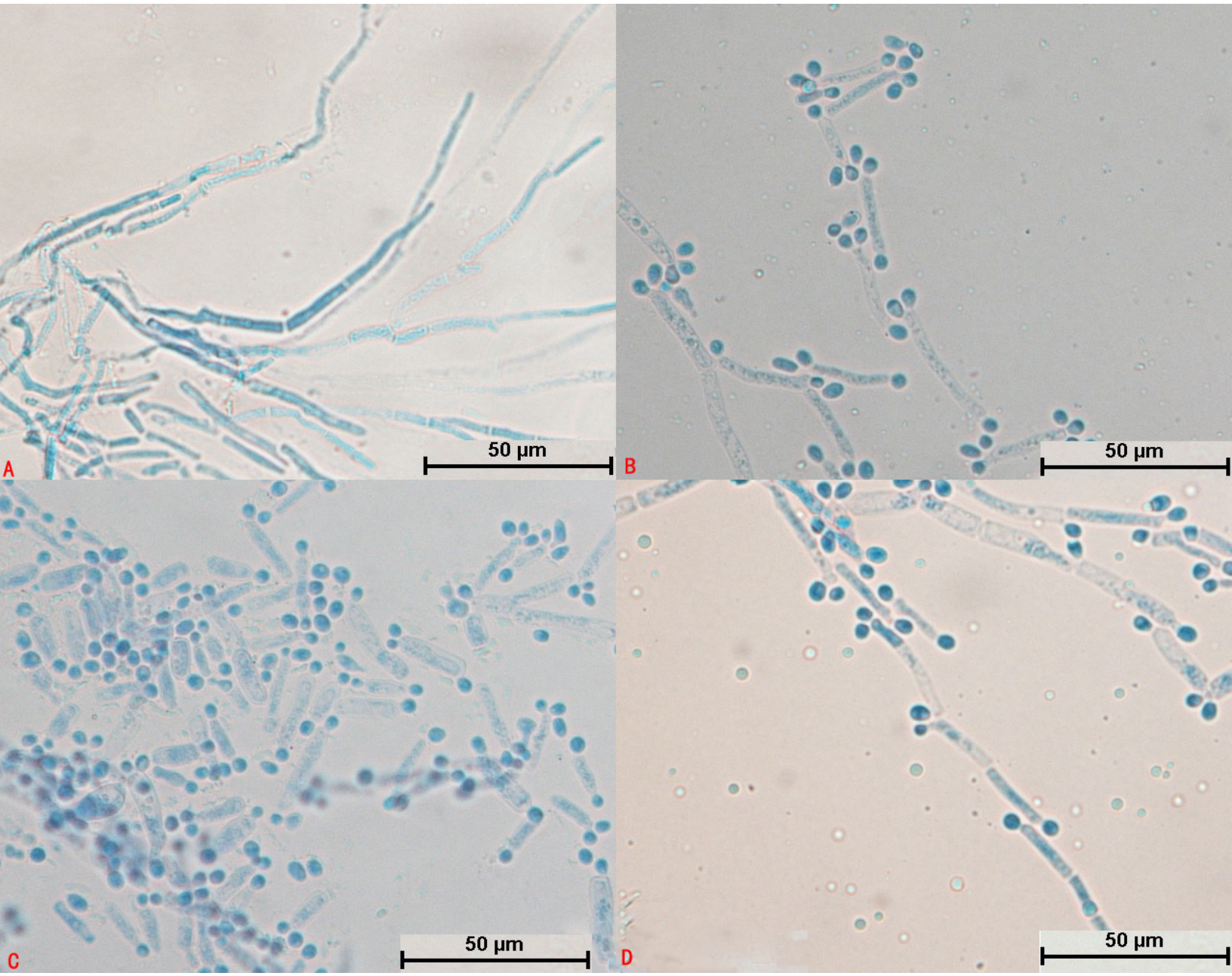
A
50 µm
B
50 µm
C
50 µm
D
50 µm

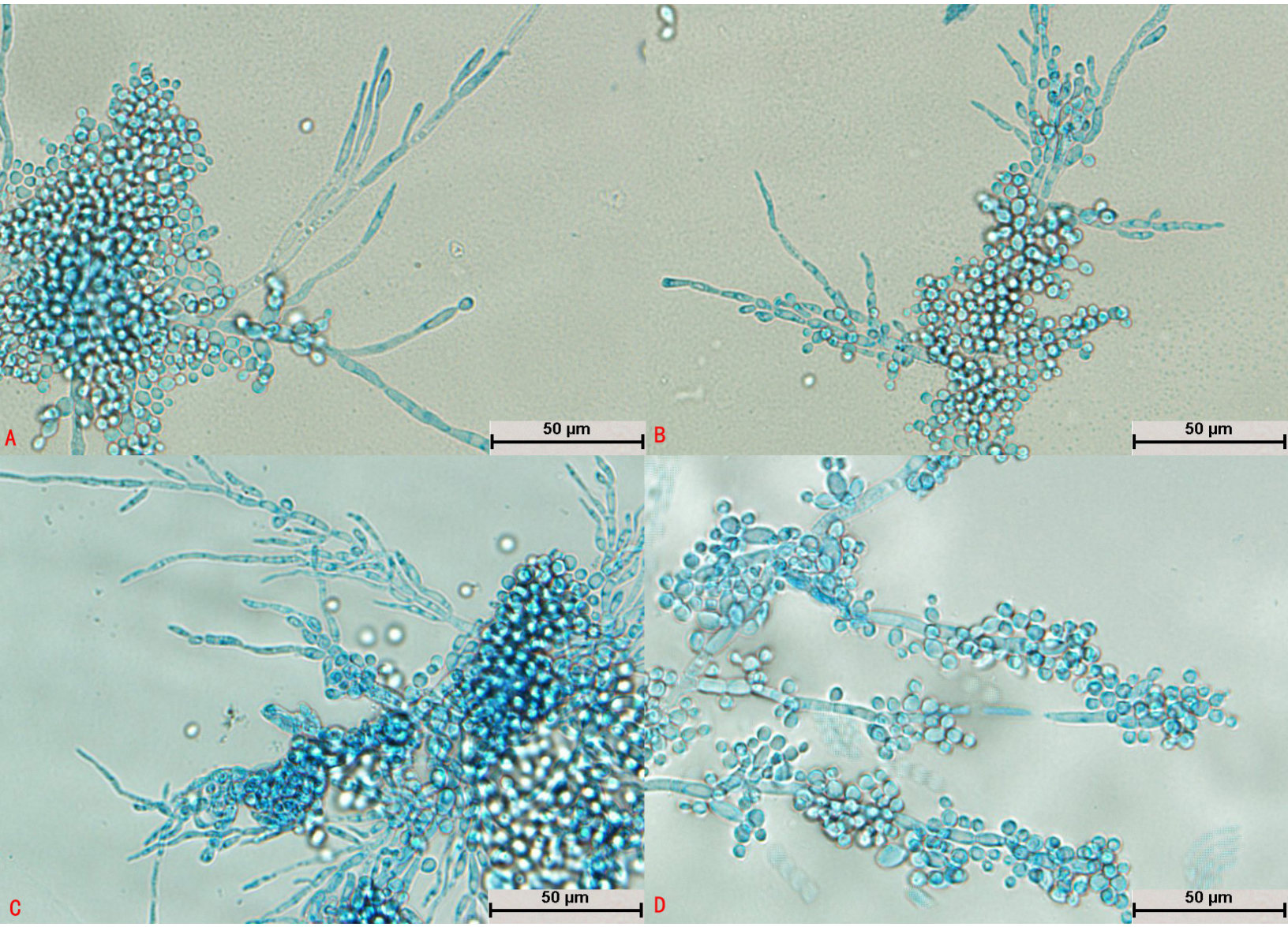
A
50 µm
B
50 µm
C
50 µm
D
50 µm

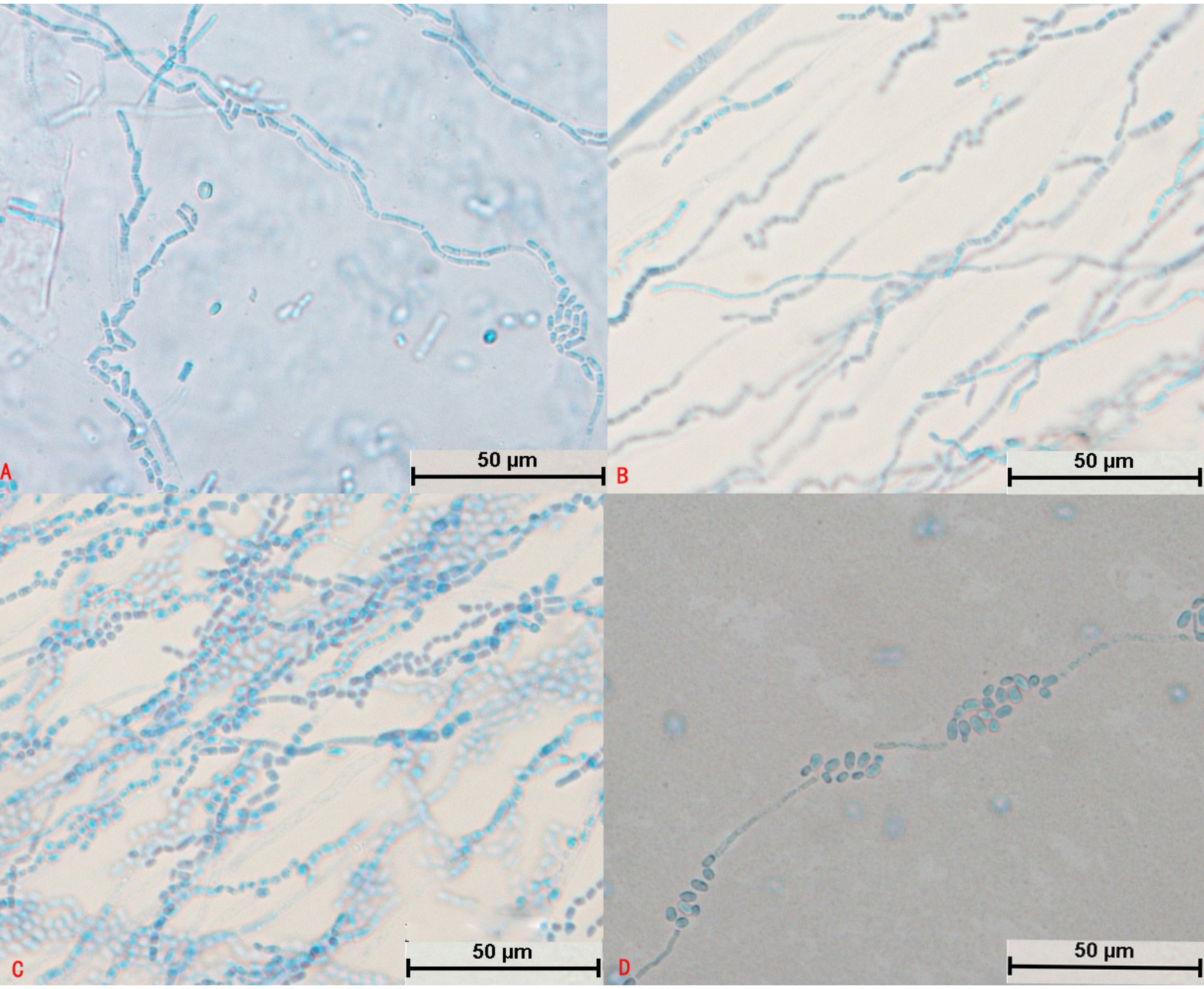
A
50 µm
B
50 µm
C
50 µm
D
50 µm

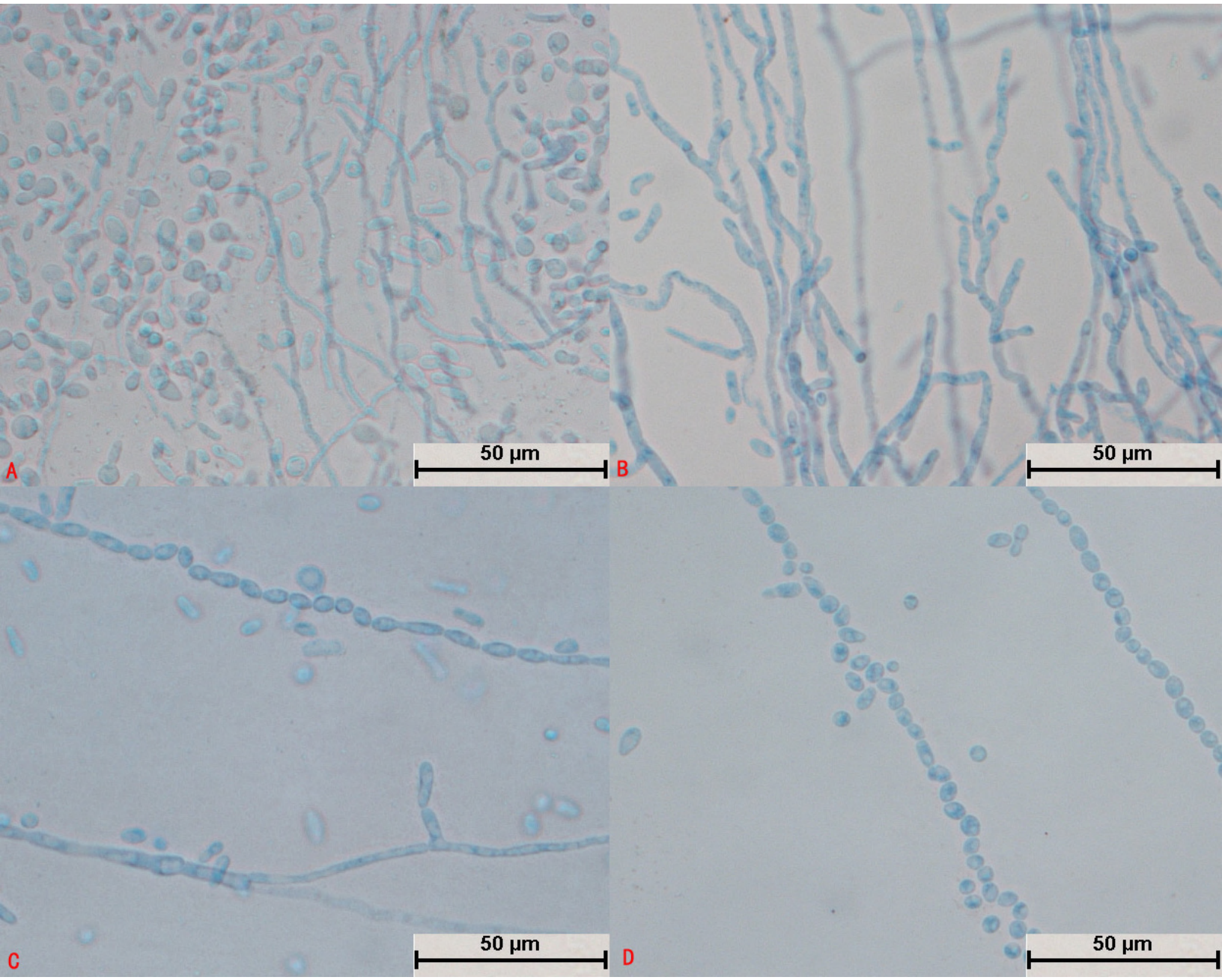
A
50 µm
B
50 µm
C
50 µm
D
50 µm

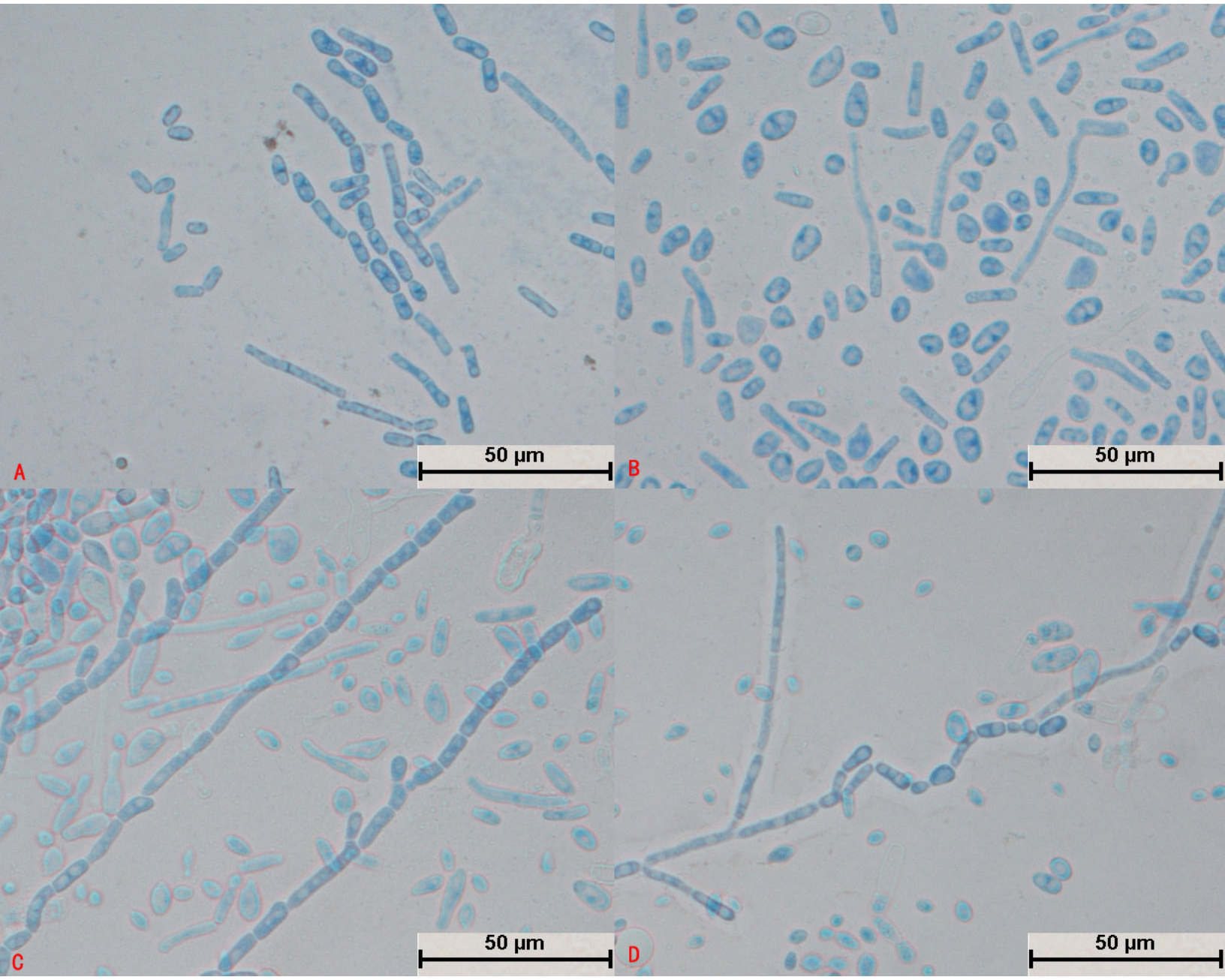
A
50 µm
B
50 µm
C
50 µm
D
50 µm

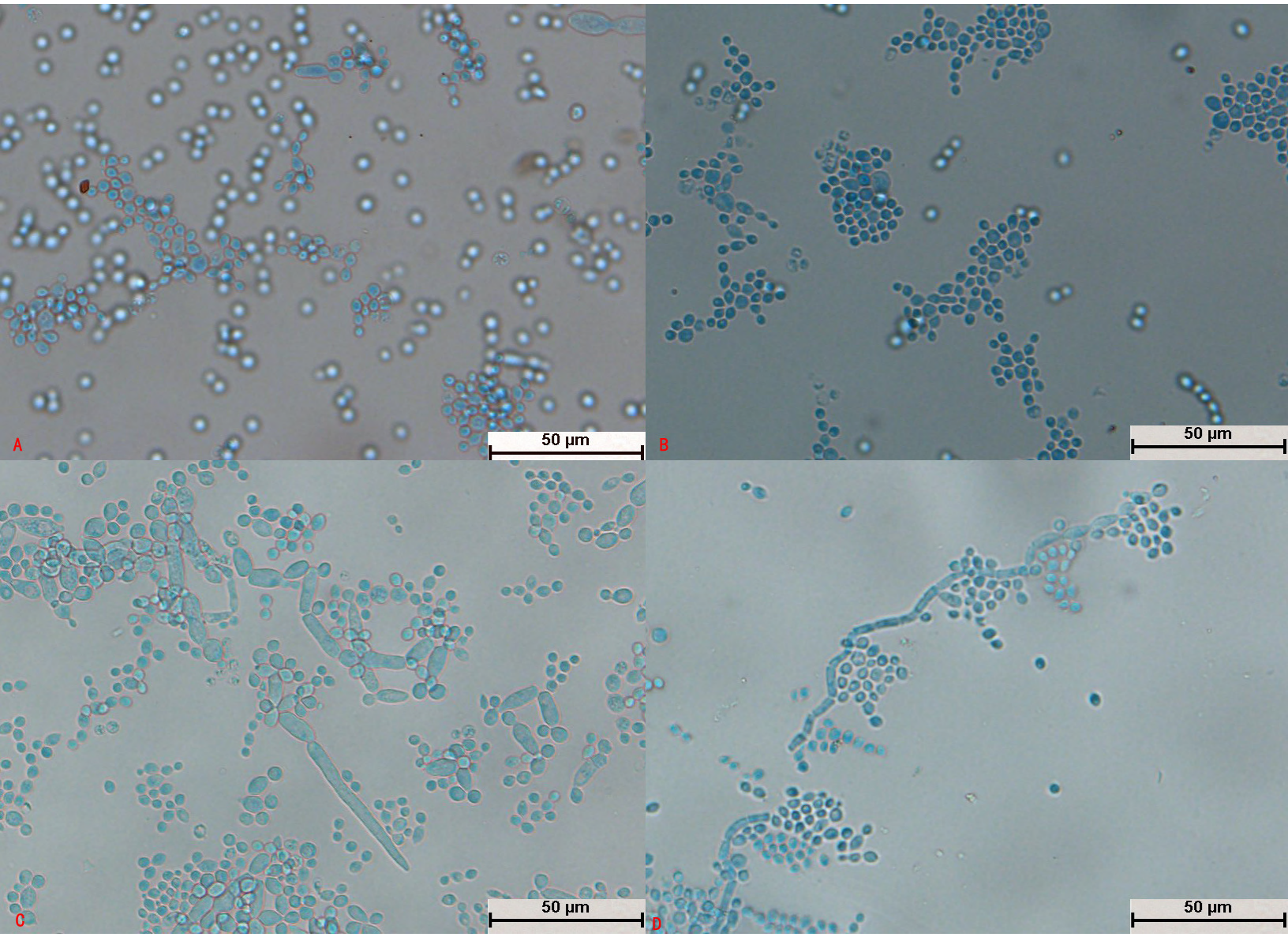
A
50 µm
B
50 µm
C
50 µm
D
50 µm

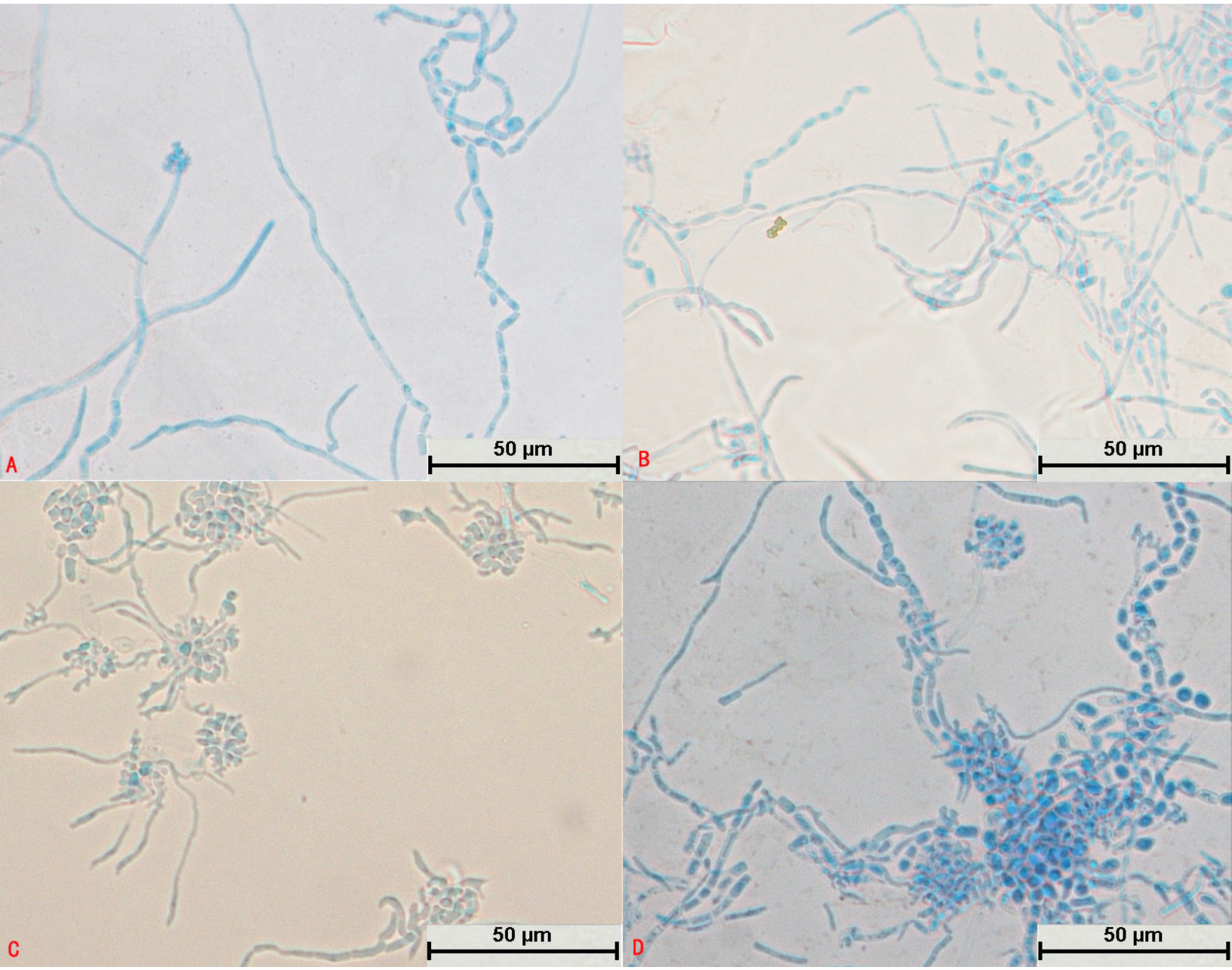
A
50 µm
B
50 µm
C
50 µm
D
50 µm

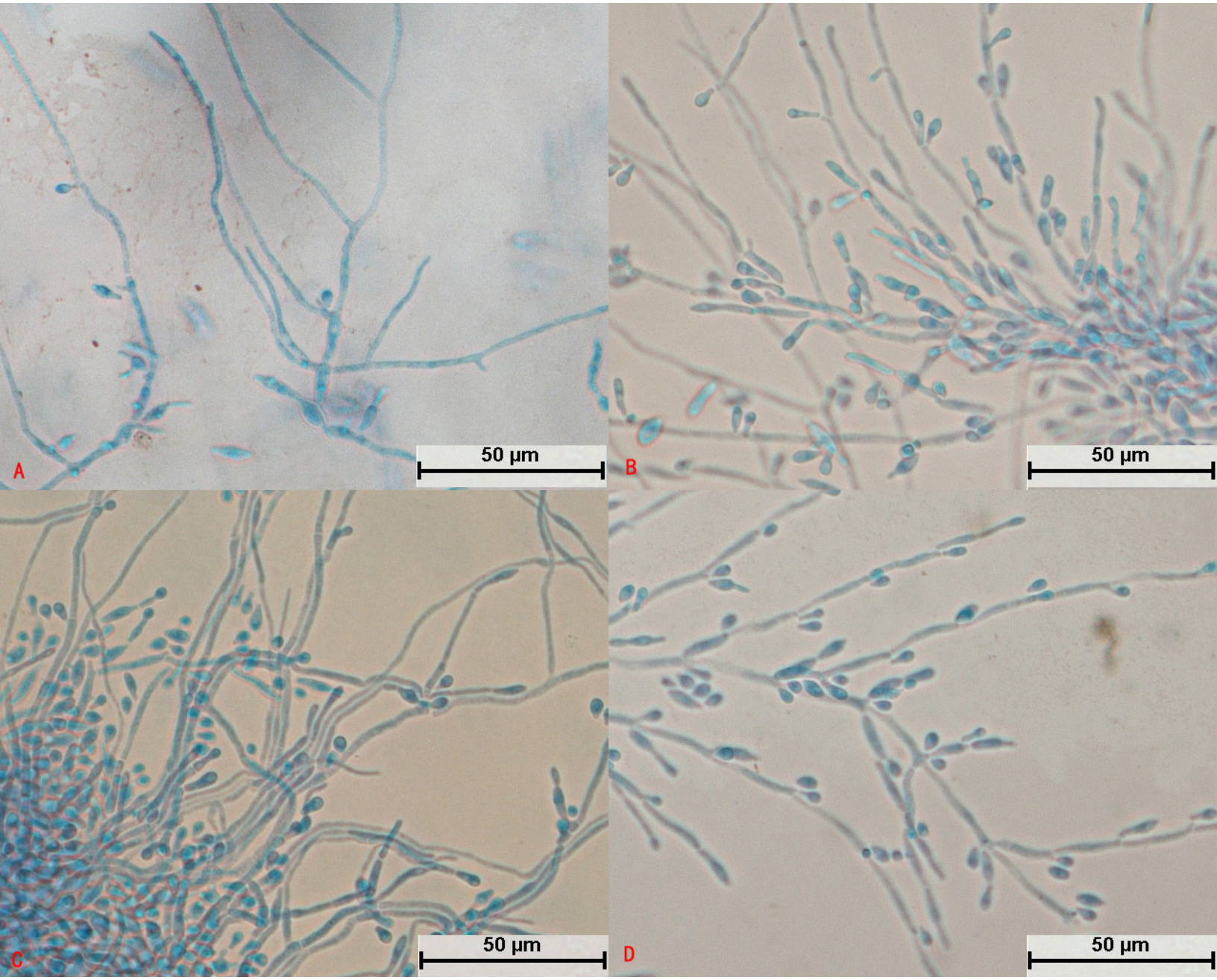
A
50 µm
B
50 µm
C
50 µm
D
50 µm

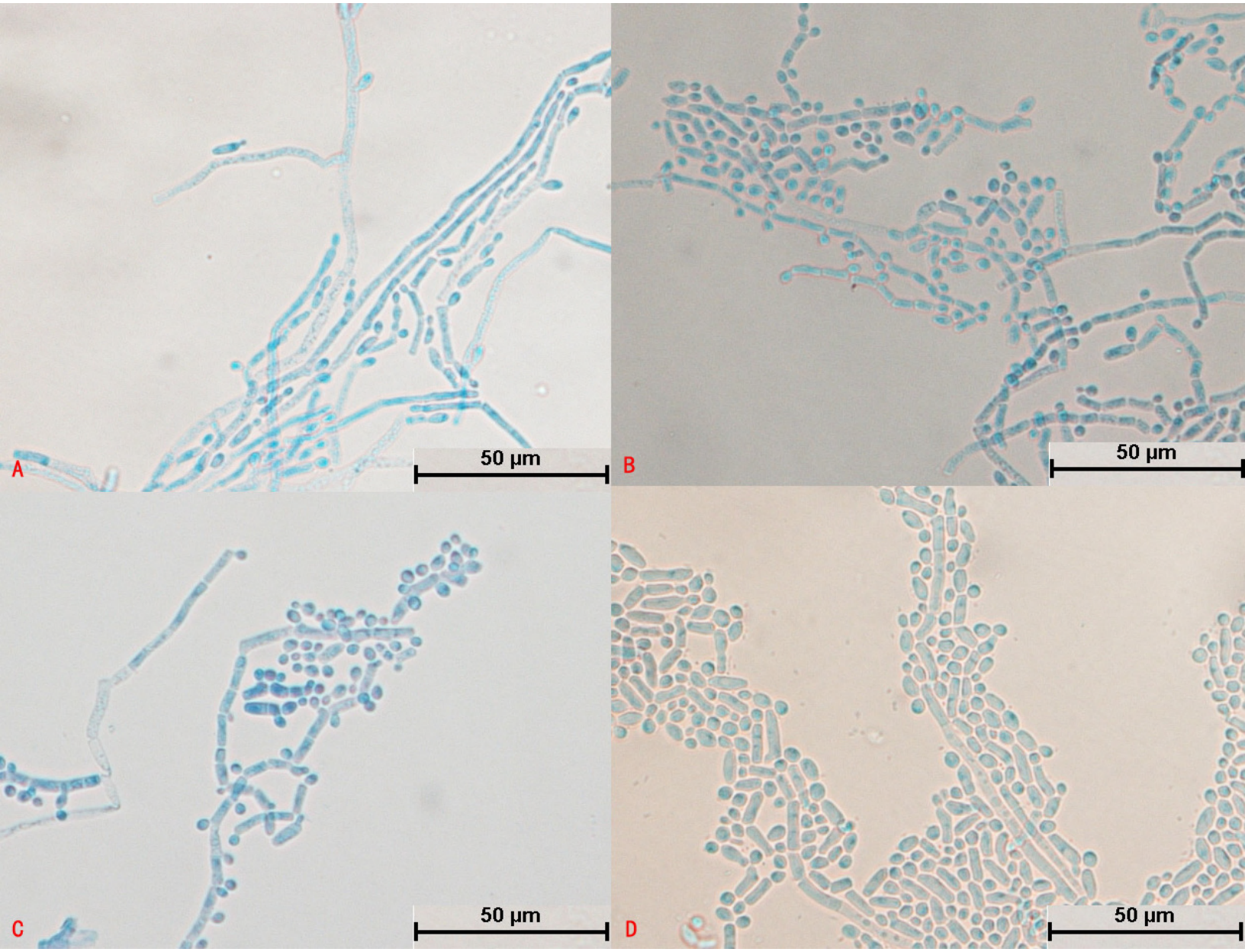
A
50 µm
B
50 µm
C
50 µm
D
50 µm

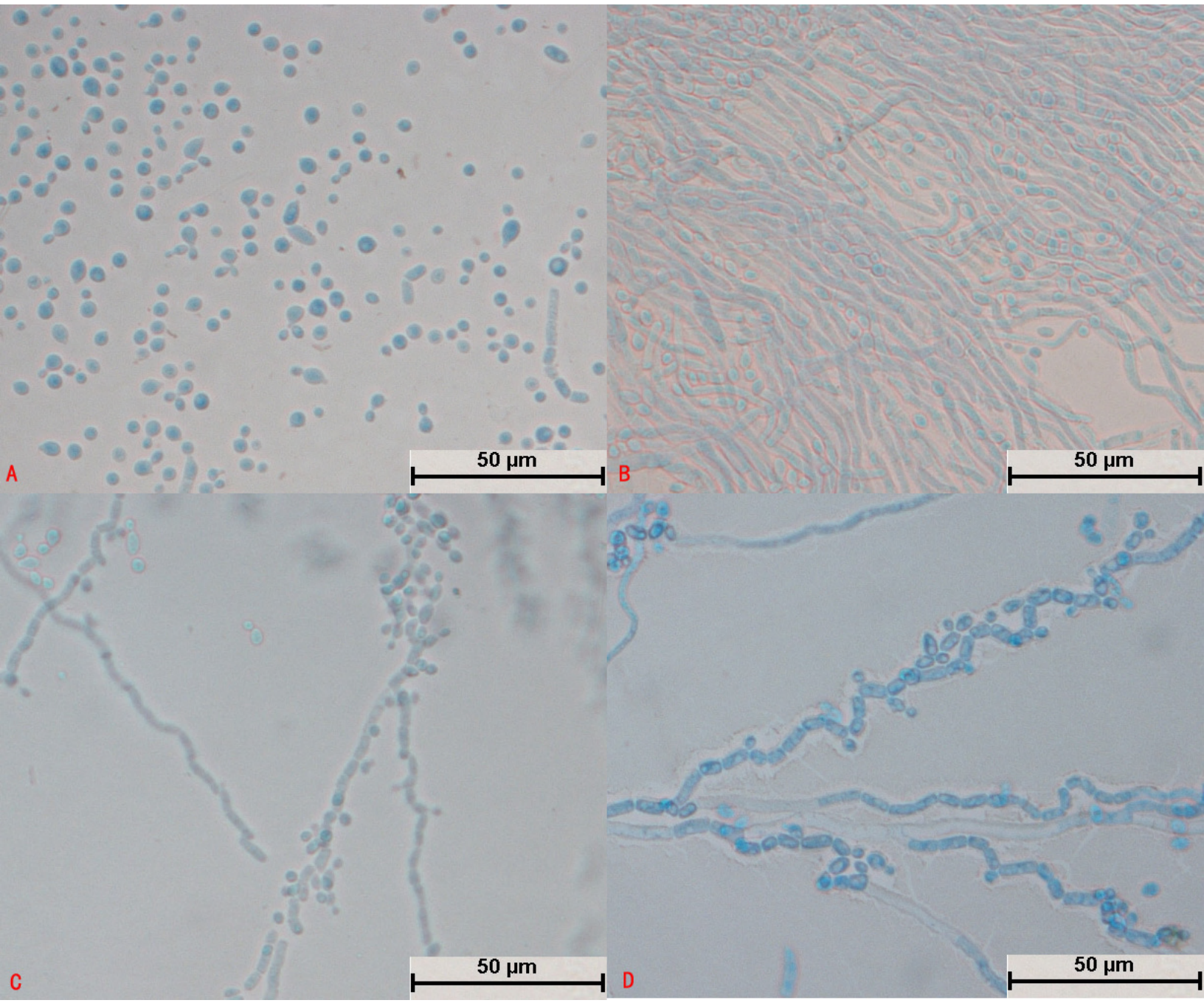
A
50 µm
B
50 µm
C
50 µm
D
50 µm

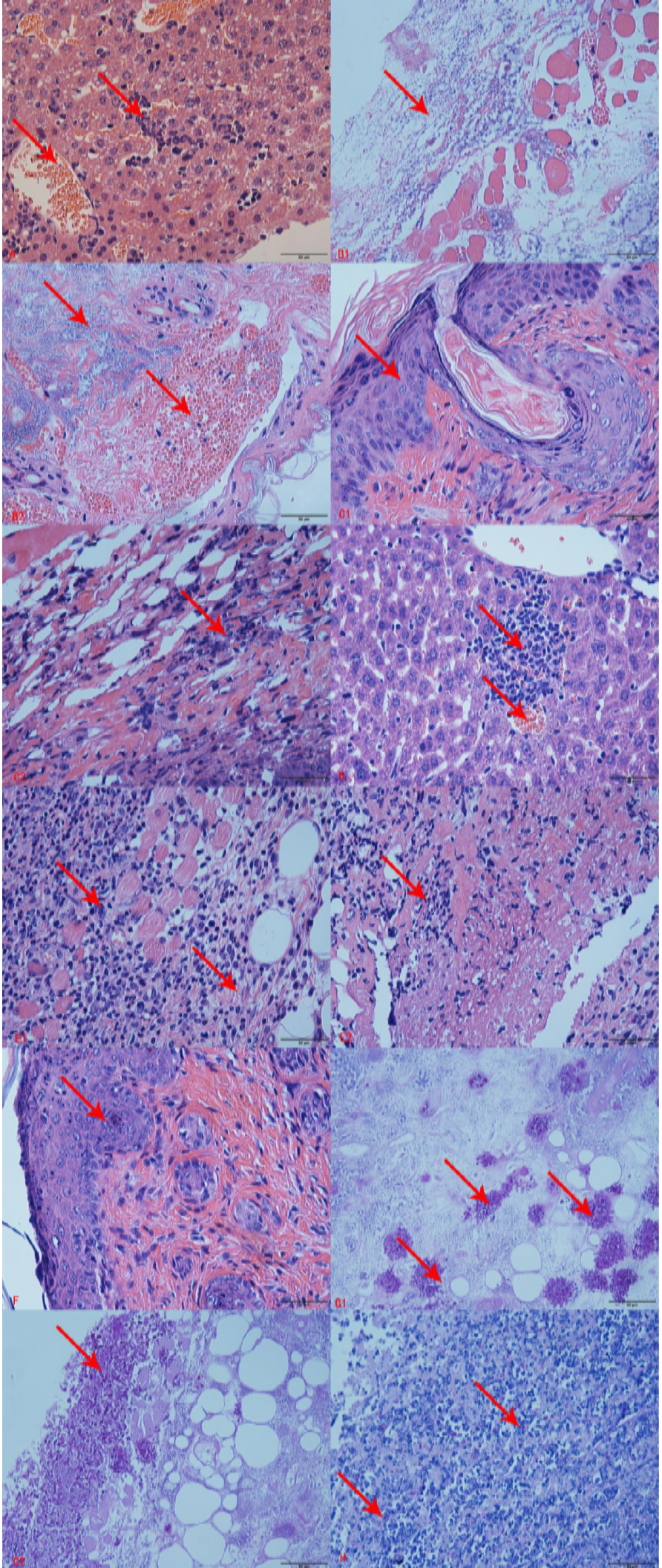
A
B1
B2
C1
C2
D1
D2
E1
E2
F
G1
G2
H